—*Danio rerio*—

Extracellular matrix and cancer cell growth in the zebrafish xenograft model

Nina Ylinen
29890
nina.ylinen@abo.fi

Master's Thesis in Cell Biology
CB00BR56, 30sp
The Faculty of Science and Engineering ÅAU
Supervisor Ilkka Paatero Ph.D. UTU, Guillaume Jacquemet Ph.D. ÅAU
Turku BioScience Center

Åbo Akademi University
2023

Åbo Akademi

Abstract

Cancer is an exponentially growing health concern worldwide. Besides genetic mutations and altered proliferation patterns, the microenvironment, and the cancer cell niche function as an essential regulator of the tumors' ability to proliferate and metastasize. While *in vitro* culturing including spheroid and organotypic models have provided valuable insight into cancer biology, their ability to recapitulate and accurately predict *in vivo* outcomes is limited. The inconsistency between results obtained in *in vitro* studies versus *in vivo* studies has led to a vast majority of promising treatments failing when expanded to animal trials and clinical testing. In contrast to the murine xenograft model, the zebrafish offers many benefits regarding space requirements, cost-effectiveness, and ethical considerations. Therefore, zebrafish avatars hold promise for drug screenings on patient-derived xenografts and expansion potential in the field of personalized medicine.

This project aimed to investigate alternative methods for MDA-MB-231 mCherry tumor cell detection beyond fluorescent microscopy, as well as to explore how extracellular matrixes (ECMs), namely Grow-Dex®, Matrigel®, PureCol® (collagen), Fibronectin, and Gelatin, could be utilized to affect the survival, growth, and migration of cancer cell xenografts in zebrafish embryos. Using human mitochondrial DNA as the target sequence for qPCR demonstrated adequate sensitivity for detecting MDA-MB-231 mCherry tumor cells from single embryo samples. Compared to the established protocols done by fluorescent microscopy, the method as such was not deemed adequate but would need further standardization and validation to be considered applicable. The experiments combining MDA-MB-231 mCherry tumor cells with ECMs followed up with fluorescent imaging indicate that Matrigel®, PureCol®, and Gelatin positively affect the size of the primary tumor transplant. The ECMs did not, however, affect the number of cells dissociating from the xenograft injection site, nor the rate at which the tumor grew over the incubation period. In conclusion, while no additional benefit from ECMs on fold-change or changes in migrating cells could be observed, the increased success rate and decrease in variability of the xenografts could advocate for the usage of ECMs in conjunction with the zebrafish cancer xenograft model.

Table of Contents

Abbreviations

CAF- Cancer-Associated Fibroblast

DMEM- Dulbecco's modified Eagle's medium

ddPCR- digital droplet Polymerase Chain Reaction

dpf- days post-fertilization

dpi- days post-injection

ECM- Extracellular Matrix

EGF- Epithelial Growth Factor

EHS-sarcoma- Engelbreth-Holm-Swarm sarcoma

ER- Estrogen Receptor

FBS- Fetal Bovine Serum

GAPDH- Glyceraldehyde 3-Phosphate Dehydrogenase

GFP- Green Fluorescent Protein

GNP- Gelatin Nano Particles

HNSCC- Head and Neck Squamous Cell Carcinoma

Her2- Human Epithelial Growth Factor 2 Receptor

il2rga- Interleukin-2 Receptor Gamma A

NSG mice- Nod Scid Gamma mice (see glossary)

PBS- Phosphate Buffered Saline

PDX- Patient-Derived Xenograft

PR- Progesterone Receptor

prkdc- Protein Kinase DNA-activated catalytic polypeptide

PTU- 1-phenyl 2-thiourea

qPCR- Quantitative Polymerase Chain Reaction

siRNA- Small Interfering RNA

TAM- Tumor-Associated Macrophage

TME- Tumor Microenvironment

TNBC- Triple-Negative Breast Cancer

TPO- Thyroid Peroxidase

VEGF- Vascular Endothelial Growth Factor

Glossary

Autograft- Transplantation of one's own cells

Allograft- Transplantation of cells between genetically different individuals but of the same species

Heterotopic transplant- Transplanting cells of one tissue type to a different tissue type

Homologs- Gene alleles with similar function

MDA-MB-231- Aggressive breast cancer cell line from mammary ductal epithelia cells (adenocarcinoma)

Morpholino- A synthetic oligonucleotide with normal bases, but a backbone of methylene morpholine rings. Used to bind and modify various gene functions

NSG mice- NOD Scid Gamma, a strain of immunodeficient laboratory mice commonly used in engraftment and immune response studies. Lacks T-cells, B-cells, and NK-cells and has reduced macrophage and dendritic cell activity

Pleomorphic- The ability of a micro-organism or cell to shift appearance and behavior in response to its environment

Orthologs- Genes that have similar functions across different species

Orthotopic transplants- Transplanting of cells from corresponding tissue type

Xenograft- Transplantation of cell material from a different species

1 Introduction

Cancer is one of the top three leading causes of health-related deaths globally. As the prevalence grows exponentially, the urgent need to find novel remedies and cost-effective interventions is steadily rising. The multifaceted characteristics of tumor cells result in a considerable degree of heterogeneity in their sensitivity to the treatments at hand today. Understanding the underlying causes, and sharing the gathered information and expertise, are highly universal interests given the considerable economic burden caused to the healthcare systems worldwide.

Many researchers work with identifying the pathways by which the cancer cells survive and expand in numbers, giving rise to medicines and targeted therapies intervening with specific functions in these cells. Often, however, a tumor possesses a multitude of altered gene expression patterns whereby genetic mapping can become expensive and laborious. The 2D in vitro chemosensitivity assays based on pharmacogenetics have been used to evaluate drug efficacy on patient biopsies. Still, the results obtained with these methods are limited when implemented in patient care (Costa et al., 2020). Patient-derived tumor organoids were considered a huge breakthrough regarding the ability to mimic and preserve the behavior of tumors, hence being considerably superior in their aptness to accurately predict patient outcomes (Costa et al., 2020). The common limiting denominator of these *in vitro* methods remains the unreliable predictive power and the long time needed to generate the cell cultures and organoids (Costa et al., 2020). From the perspective of the zebrafish cancer xenograft model, the enhanced mimicry of the complexity of the tumor habitat, and the possibility to monitor toxicity and tumor suppression simultaneously can be seen as a significant advantage. Zebrafish embryo avatars are used in research to predict the efficacy of drug therapies against different commercial tumor cell lines as well as PDXs (Patient-Derived Xenografts) (Al-Samadi et al., 2019; Costa et al., 2020). Ideally, the zebrafish cancer model could be expanded to clinical use for direct screenings for growth-suppressing therapy alternatives on PDXs implanted into a battery of zebrafish embryo avatars.

Expanding the knowledge of factors affecting the xenograft and finding ways in which the tumor cells would reliably thrive would be beneficial for expanding drug screenings in zebrafish embryos. Translating and predicting cell behavior from one cell type to another would require a wider repertoire of different tumor cell strains tested in a wider range of *in vivo* systems. Alterations in ECM building blocks could provide additional information on how to advance protocols for zebrafish xenografting, as the tumor niche plays such a crucial role in tumor survival in both real-life and laboratory settings.

Improvements in the zebrafish xenograft model could ultimately help in breaching the gap between what today presents a profound problem in biomedical research: namely that many promising *in vitro* effects fail to coincide with that which is eventually observed when applied in *in vivo* systems. Tailored and targeted multiple-pathway treatments being the best approach according to the current understanding of cancer therapy, the zebrafish has the potential to be more widely applicable for *in vivo* screening purposes on PDXs in the field of personalized medicine.

2 Literature Review

2.1 Zebrafish as a model organism in Research

The zebrafish —*Danio rerio*— a small freshwater fish, has been an object of various scientific applications since the first tests performed by George Streisinger in the 1960s (Astell & Sieger, 2020; Bradford et al., 2017). Zebrafish research at this time was simple, observing embryogenesis and testing how early development is affected by different interfering agents (Bradford et al., 2017). This method of toxicity screening is still widely used today, but zebrafish research has extended to include various applications relying on genetics and molecular biology (Bradford et al., 2017). New inventions in the field of molecular biology have been used to expand the zebrafish model to mimic different mutations and disease states in humans, cancer being one of them (Astell & Sieger, 2020; Nakayama et al., 2022). Knockouts, knockdowns, and knock-ins facilitated by CRISPR-Cas9 techniques, morpholinos, and interfering RNAs can be used to track how the silencing of genes and proteins affects the zebrafish. In addition, the elimination of pigment genes in the opaque Casper strain zebrafish, and the possibility to transgenetically insert tissue-specific fluorescence, have made the Casper strain zebrafish a prevalent subject for live imaging (White et al., 2008). In conjunction with the rapidly developing state-of-the-art powerful microscopy and imaging technologies, the zebrafish model provides a valuable tool for observing various biological processes in real-time.

The benefits of using zebrafish include low cost and easy maintenance, and the transparent zebrafish embryo enables early development studies ex-utero (Hason & Bartůněk, 2019). Several mutated phenotypes correlating with the same gene dysfunctions found in human disease have been developed (Hason & Bartůněk, 2019). Genetic mutations and incorporation of, for example, reporting markers are more accessible to conduct than in other higher-order vertebrates. The zebrafish has a genome of roughly 26,000 protein-coding genes and most organ systems that correspond to that of humans. The zebrafish genome has 72% orthology with the human genome, and up to 82% orthology for disease-causing genes (Howe et al., 2013).

Producing large amounts of offspring in a short period of time makes the zebrafish ideal for large-scale toxicological studies and various pre-clinical screenings of potential therapeutic small-molecule compounds (Bradford et al., 2017). Up to 200 offspring per week of "genetically similar siblings" is a substantial benefit compared to the murine models. In the future, this could offer a possibility for personalized medicine, especially useful in conditions like cancer, with a wide range of variations regarding the causative mutations. In addition, the rapid development of the zebrafish makes any induced effects manifest at a fast pace.

In large-scale screening, the substance under investigation can be directly administered in the water of the fish, embryo, or larvae. The zebrafish is comparatively easy to keep under steady concentrations when evaluating drug efficacy; this in contrast to murine models where substantial liver clearance often results in unstable blood concentration of the active substance (L. Chen et al., 2017). Pharmacokinetics can be adjusted by tittering the concentration in the water, and absorption happens directly through the gills, the buccal cavity, and the skin (X. Chen et al., 2021). Specific organs like the liver and the vasculature of an optically transparent zebrafish can be genetically modified to express fluorescent proteins, and labeled nanomedicines can be visualized in real-time for biodistribution studies (X. Chen et al., 2021). Monoclonal antibodies (cetuximab and bevacizumab) have been tested in this fashion against specific zPDX (Zebrafish Patient-Derived Xenografts), and the results have been promising, generating similar effects in the actual patients as in the zPDX model (X. Chen et al., 2021).

Over the past 40 years, the zebrafish has established a firm foothold as a model organism in research. The scientific community has collaborated since 1994 to build a database, the zebrafish information network ZFINs (https://zfin.org), supporting zebrafish enthusiasts and accelerating the speed at which better models and methods are developed and shared among colleagues. ZFINs is part of a larger organization for researchers working with different model organisms, together forming what is called the Alliance of Genomic Resources. Here scientists working in different fields with different model organisms aim to promote human health by better understanding the genetics and cellular mechanisms underlying health and disease.

2.2 The Extracellular Matrix and the Tumor Niche

The ECM (Extracellular Matrix) is a complex microenvironment surrounding all living cells (Mouw et al., 2014). It is built out of over three hundred different proteins, where the exact composition depends on the tissue it is part of (Lepucki et al., 2022) (Figure 1). The glycoproteins, together with fibrous proteins like collagen, elastin, laminins, and fibronectins, occupy the main volume of the ECM, providing each tissue a specific stiffness and rigidity (Insua-Rodríguez & Oskarsson, 2016; Karamanos et al., 2021; Mouw et al., 2014; Schaefer & Schaefer, 2010). Together with several enzymes and signaling molecules, the cell can mechanically and chemically sense and interact with its surroundings. A myriad of signaling molecules and immune cells constantly guard and monitor the extracellular space to maintain a dynamic homeostasis (Karamanos et al., 2021). Cancer alters the cell's gene expression and intracellular functions, but changes in the ECM and the tumor-niche interactions are by today's understanding considered equally significant for cancer progression (Paolillo & Schinelli, 2019).

In cancer, the normal function of the ECM is high-jacked to over time transform into a so-called TME (Tumor Microenvironment) (Quail & Joyce, 2013). Fibroblasts, producing collagen and maintaining the structure of the ECM, enhance their activity. The fibroblasts surrounding the tumor transform into CAFs (Cancer-Associated Fibroblasts), making more firm and rigid structures (Quail & Joyce, 2013). The dysregulated protease function in the TME remodels the matrix, paving the way for the tumor to expand and for cancer cells undergoing EMT (Epithelial-to-Mesenchymal Transition) to escape their primary location. EMT is essentially a reversal of cell differentiation and the programming of cell fate, which occurs after gastrulation when the migration of the different cell layers is completed (Sadava et al., 2012; Weinberg, 2014). Fibroblasts differentiating to myofibroblasts and CAFs enhance the secretion of growth factors, hormones, and chemokines, attracting more T-lymphocytes and macrophages further promoting cancer growth (Walker et al., 2018). The macrophages found accumulating at tumor sites transform into TAMs (Tumor-Associated Macrophages), which can be divided into M1 and M2 types of macrophages (Quail & Joyce, 2013; Travnickova et al., 2021). Early in the tumor progression, M1-type

macrophages promote adequate immune response by trying to maintain pro-inflammatory cytokines with anti-tumorigenic effects. However, over time the balance shifts to progressively be dominated by M2-type macrophages which do the opposite by promoting anti-inflammatory cytokines, downregulating sufficient immune responses, and thereby reinforcing tumor growth (Quail & Joyce, 2013). The exact mechanisms of what factors contribute to the shift of macrophage function are poorly understood (Quail & Joyce, 2013).

Contact inhibition normally stalls cell proliferation when a certain number of cells is established. Cancers originating from epithelia (carcinomas) typically undergo EMT. This is characterized by the loss of cellular polarity, the loss of cell-cell junctions, and the loss of epithelial markers like E-cadherin, all crucial for contact inhibition to operate (Paolillo & Schinelli, 2019). Instead, the cells start expressing mesenchymal markers: N-cadherin, fibronectin, and vimentin. This change eventually leads to cancer cells breaking loose from the original location and start wandering off from the site they are supposed to be a part of (Paolillo & Schinelli, 2019).

"90% of cancer deaths are caused by metastasizes" is a slogan repeated to such an extent that it has become a "fact" not only among the layman public's eye but among health professionals as well (Dillekås et al., 2019). Although some resources argue that this statement is to some extent exaggerated (Dillekås et al., 2019), the prognosis for any cancer is unarguably highly coupled with its metastasizing potential (Astell & Sieger, 2020). Tumors prone to dissociate and intravasate from the primary tumor, move via the bloodstream or lymphatic system, and extravagate and inhabit a new niche, worsen the disease prognosis significantly (Astell & Sieger, 2020). The cascade of escape is not exclusively dependent on the cell's internal happenings but relies on numerous shifts in extracellular microenvironmental factors (Vitale et al., 2022). The pro-tumorigenic niche embedded with the dysregulated immune cells is pivotal for the metastasizing strategies to be successful (Quail & Joyce, 2013). The stromal cells, leucocytes, and other immune cells fail to recognize the "altered self". Instead, they adopt a composition that favors the survival and proliferation of the tumor (Quail & Joyce, 2013). Infection and chronic inflammation are strongly associated with increased risk for tumor growth. As early as 1863, Rudolf Virchow suggested that cancer could be a consequence of failed cell metabolism and dysregulated immune

response following a prolonged condition of low-grade inflammation when he observed the elevation of leucocyte infiltration in cancerous tissue (Quail & Joyce, 2013).

One field of cancer research focuses on the study of angiogenesis and the cancer cells' enhanced expression of VEGF (vascular endothelial growth factors). Upregulated expression of VEGF accelerates neovascularization of the tumor area, ensuring the supply of oxygen and nutrients to the tumor site (Lee et al., 2009). This has been utilized in cancer treatments aiming to inhibit the neovascularization of the tumor site. The tumor mass, however, depending on size, often suffers from a chronic state of moderate hypoxia. In this context, the inhibition of VEGF, combined with the cancer cells' disorganized and leaky vasculature, can counterproductively lead to accelerated metastatic tendencies, especially as the tumor grows more prominent and is exposed to higher degrees of oxygen deprivation (Lee et al., 2009).

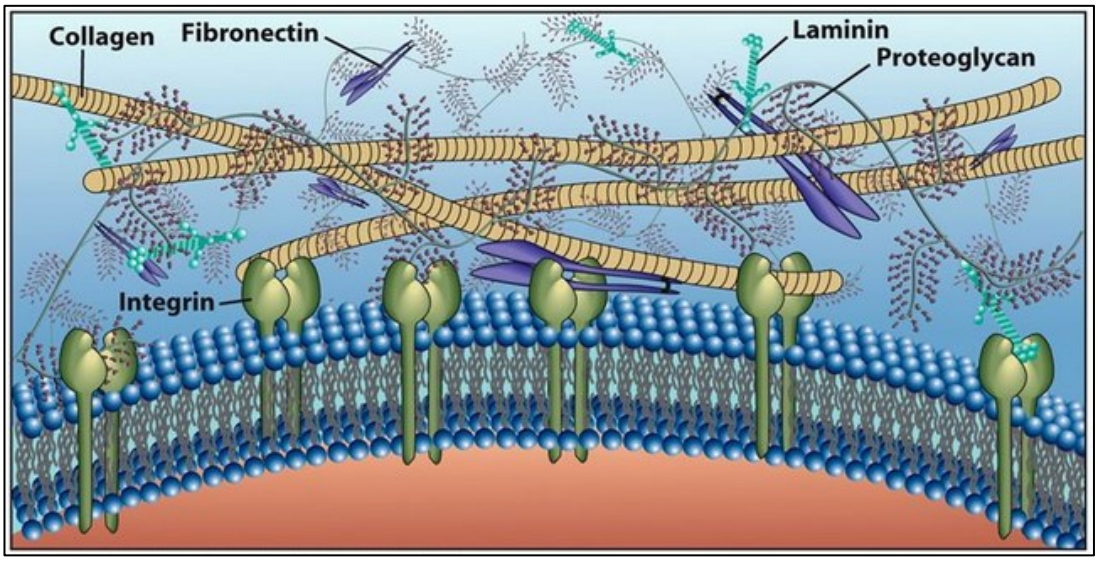

Figure 1: A simplified version of the ECM network (Extracellular Matrix). Collagen, fibronectin, laminin, and proteoglycans occupy the main volume of the ECM, while integrins function as an essential link and signal deliverer between the ECM and the cell cytosol. Integrins participating in the formation of migratory appendixes known as filopodia, are interconnected with intracellular signaling pathways and are highly coupled with and driven by the prevailing composition of the niche. (Figure borrowed from Cell and Molecular Biology: Concepts and Experiments, by Gerald Karp, with permission from ©2008 John Wiley& Sons).

2.3 Extracellular Matrixes in Cell Culturing and *in vivo* Experiments

In laboratory circumstances, many cells are anchorage-dependent and grow poorly without an adequate substrate or matrix for attachment. Cell lines in culture produce some matrix for themselves, but especially poorly growing cells can be stimulated by providing the culture with both nutrients and different ECM substitutes. Xenografts, often challenging to grow in a recipient animal, can also benefit from additional building blocks supporting cell sustenance (Benton et al., 2011). Even though many of these ECM techniques used *in vitro* have successfully been implemented and utilized in the murine xenograft models, the generally available literature suggests that the adoption of these techniques into the zebrafish xenograft model remains limited and has not become standard practice.

2.3.1 PureCol® collagen

Collagen is, by volume, the most abundant component of the natural ECMs with 28 different collagen types being identified to this date (Gordon & Hahn, 2010; Insua-Rodríguez & Oskarsson, 2016). Each collagen microfibril comprises three helical polypeptide chains, assembling into homo- or heterotrimeric helixes (Gordon & Hahn, 2010; Walker et al., 2018). The microfibrils further arrange to form thicker fibers with the aid of decorins, biglycans, and hyalectans, and together with laminins and fibronectins they form complex branched networks, maintaining the appropriate rigidity and cell support of each tissue (Walker et al., 2018).

PureCol® is a cell culture supplement derived from bovine hide, containing 97 % type I collagen and the remaining part comprising mainly type III collagen. It comes as a water-soluble atelocollagen, a modified form of collagen where the C- and N- terminus telopeptides of the collagen polypeptide chain have been enzymatically removed using pepsin (Nimesh, 2013). The enzymatic removal of these moieties aims to mitigate the antigenicity and reduce the provocation of immune responses associated with the usage of certain types of collagens (Nimesh, 2013). In addition to collagen being

utilized as a matrix coating for *in vitro* plates and as a scaffold for cellular growth in 3D cultures, different formulations of collagen exhibit versatile applications in *in vivo* contexts, including bio coatings for medical devices for surgical and prosthetic purposes, as well as a tool for drug delivery systems (Hanai et al., 2012; Nimesh, 2013). The positive charge of the atelocollagen attracts positively charged nucleic acid chains, and once solidifying in physiological temperatures, it protects the gene material from immunological responses and enzymatic degradation. In mouse models, atelocollagen shielding has successfully been used to deliver antitumorigenic proteins and mRNA *in vivo* (Nimesh, 2013). As an alternative to plasmid transfection and viral vectors with their limits for *in vivo* use, siRNA (small interfering RNA) can be delivered to both dividing and non-dividing cells in a biocompatible delivery system provided by atelocollagen (Minakuchi, 2004). In regard to zebrafish xenografting and the increasing interest in utilizing siRNA as therapeutic agents for suppressing oncogenic driver genes, collagen has the potential to serve a dual role. In addition to possibly providing support for the engrafted PDX in zebrafish, collagen could also be used to investigate the effects and delivery of siRNA in an *in vivo* setting.

2.3.2 Gelatin

Gelatin is a widely used biomaterial for coatings in cell culture plates, dishes, and flasks (Afewerki et al., 2019). The benefits of gelatin include adhesion support, ECM mimicry, high biocompatibility with a wide range of cell types, and low antigenicity (Afewerki et al., 2019). Gelatin is refined by irreversible collagen denaturation from collagen-rich animal parts, namely bone, skin, and tendons (Miladinov et al., 2002). The raw material for gelatin production is often obtained from rendering plants as a by-product of animal slaughter, primarily from porcine and bovine sources for pharmaceutical purposes. However, poultry, such as chicken and turkey, is also utilized in gelatin production (Miladinov et al., 2002). The gelatin is extracted by acidic or alkaline hydrolysis (type A or type B gelatin respectively), breaking down the collagenous polymers of either skin/tendons or bone (Afewerki et al., 2019).

Similar to collagen, gelatin can be used for enhanced drug delivery. Hydrophilic and hydrophobic substances can be packed in GNPs (Gelatin Nano Particles) for targeted and prolonged drug release (Su & Wang, 2015). Hydrogels formed by combining gelatin with polysaccharides like hyaluronan, chitin, etc., have been utilized for cell culture applications, and in the field of advanced tissue engineering, composite biomaterials that integrate gelatin polymers with materials like ceramics, silk, and chondroitin sulfate have been employed to create tissue scaffolds (Su & Wang, 2015). The versatility and lucrative pricing of gelatin relative to many other commercial ECM-mimicking polymers (both natural and synthetic), make it a particularly interesting macromolecule to be utilized for developing cost-effective methods for biomedical research (Su & Wang, 2015).

2.3.3 Fibronectin

Fibronectin is the extracellular fibrous matrix glycoprotein normally secreted by the mesenchymal stromal cells, the fibroblasts (Alberts et al., 2022; Walker et al., 2018). Infiltration of fibroblasts and upregulated fibronectin expression is a typical finding in several cancer types, not least metastatic breast cancer, as the presence of fibronectin is thought to function as an essential organizer of the collagen network giving rise to the denser tissue mass of tumors (Insua-Rodríguez & Oskarsson, 2016). Fibronectin is composed of subunits encoded by one or several fibronectin genes that splice into numerous different fibronectin isoforms. It can exist in two forms: as soluble units, or as a fibrillar mesh on the cell surface (Alberts et al., 2022). Dimerization of fibronectin units relies on the formation of disulfide bridges, and the formation and organization of the fibrillar mesh are thought to depend on the close interaction with the cellular integrins breaching through the lipid bilayer of the cell membrane. The physical tension exerted by cellular integrins on fibronectin polymers leads to the stretching of the fibronectin fibrils, thereby exposing binding sites that enable the attachment of additional fibronectin units to the growing mesh (Alberts et al., 2022). Together with other matrix glycoproteins, the fibronectin isoforms form a variety of scaffolds that exhibit close interactions with collagen and a myriad of other components of the extracellular matrix (Alberts et al., 2022). Fibronectin can be viewed as one of the

organizers of, and connectors between, different players of the ECM. Cancer cells undergoing EMT, and the following metastatic migration rely on the transmembrane integrins interacting with the extracellular fibronectin network. In addition, the fibronectin-integrin interaction mediates several intracellular signaling pathways regulating the balance of survival and apoptosis. Consequently, normal cells undergo anoikis (cell death) if this connection is lost (Alberts et al., 2022). The stiffer surroundings and excess secretion of fibronectin in close proximity to the tumor are contributing factors messaging the cancer cells to keep proliferating. In 2011 Maity et al. showed that MDA-MB-231 cells grown on a fibronectin-enriched substrate expressed higher amounts of MMP-9 (Matrix Metallo Proteinase 9) and enhanced motility in wound healing assays, and speculated that this could be caused by upregulation of several integrin-dependent pathways (FAK, PI-3K, ILK, NF-κB) boosted by the "excess" fibronectin (Maity et al., 2011).

2.3.4 Matrigel® and Grow-Dex® matrix

Both Matrigel® and Grow-Dex® are matrix substitutes or imitations, developed and used for in vitro 2D and 3D spheroid and organotypic cultures. Matrigel® is an ECM substrate miming the basement membrane composition and enhancing growth, especially in epithelia-derived cells. Matrigel® is extracted from mouse EHS-sarcoma cells (Engelbreth-Holm-Swarm sarcoma) that produce copious amounts of a matrix rich in collagen IV, laminins, and several growth factors like TGF (Transforming Growth Factor) and EGF (Epithelial Growth Factor). The heterogeneous composition of Matrigel® is soluble in cooler temperatures (+4°C), but the polymers solidify at room and physiological temperatures. Various cell types of mouse model xenografts have been shown to benefit from the simultaneous administration of Matrigel®, supporting the survival and enhancing the "take" of the graft (Benton et al., 2011).

Grow-Dex® is a wood-derived (from birch) nanocellulose, a fibrillar hydrogel developed by the Finnish company UPM. It can be used as cell culture support much like Matrigel®, with the difference that synthetic Grow-Dex® does not contain any animal-derived structural components nor any naturally occurring growth factors or

nutrients. As a result, microenvironmental growth enhancing/inhibiting factors can be tailored as wished and are easier to manage and control, compared to Matrigel®, where the exact formulation is variable and highly batch specific. One benefit over Matrigel® is that Grow-Dex® is not as reactive to temperature changes, making it less demanding to handle at RT (room temperature). Conversely, though, the nanocellulose is rather glue-like in all temperatures, adding a challenge for being applicable for the nanoliter volumes required for zebrafish xenografting. Grow-Dex® being a more recent innovation and addition to the laboratory ECMs, the utilization of Grow-Dex® for *in vivo* applications in animal model xenografting is not widely available in the literature.

2.4 Zebrafish as a cancer xenograft model

The zebrafish tumor xenograft model offers a platform to monitor tumor growth, tumor cell invasion and the ability of the tumor to form micrometastases (Figure 2). All tissue transplants, even the ones that are moved within an individual (autografts) from one part of the body to another (e.g., skin cell grafting), face the problem of rejection, if the transplanted cells do not incorporate as a part of their new environment. If the cell surface markers differ substantially, the transplant is perceived as non-self, and the immune system is hasty in its attempt to eliminate the "invading" cells. This is part of the crucial protective system upholding tissue integrity, the failure of which is a hallmark of malignant cancer, where metastasizing and migrating tumor cells have been able to escape the recognition by the immune cells and consequently inhabit a new location. Allografts, transplanting cell material between individuals (of the same species), pose an even more considerable risk of tissue rejection than autografts, and the most significant immunological challenge is faced when performing xenografts (inserting cell material between different species). Xenografts can further be divided into orthotopic and heterotopic transplants. With orthotopic transplants, the inserted cells originate from the same tissue type, whereas in heterotopic transplants the cells are transplanted into a tissue different from their origin (Astell & Sieger, 2020). Transplanting human MDA-MB-231 breast cancer cells in zebrafish is in the category of heterotopic xenografting.

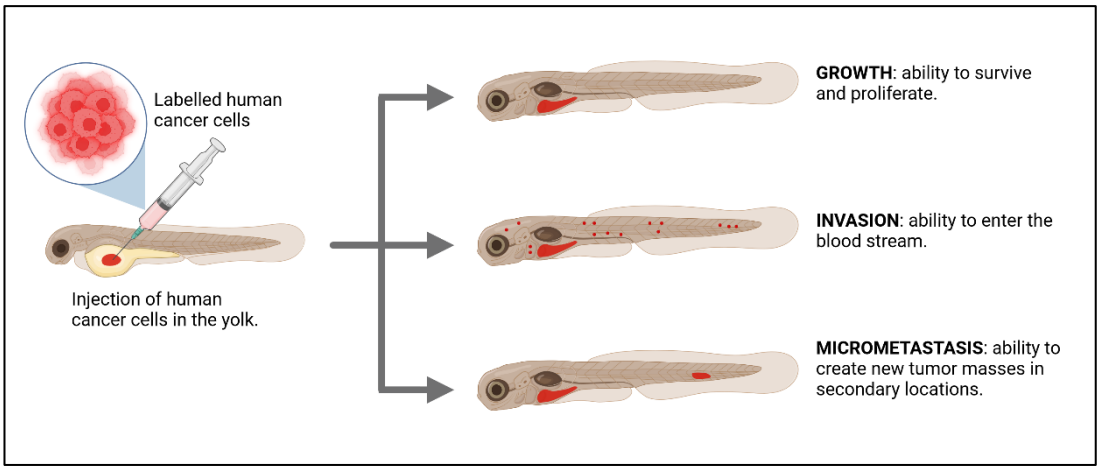

Figure 2: In the zebrafish xenograft model, the labeled cancer cells can be monitored in their ability to grow, invade, and in their ability to form micrometastatic tumor masses. Fluorescent imaging is the most common way to quantify tumors but other methods like qPCR can also be utilized. (Figure created with BioRender).

Modeling human tumors in various humanized and immunodeficient murine models has long been the golden standard of xenografting (Yan et al., 2019). Economical concerns and the growing public awareness about ethics regarding animal testing have progressively increased the pressure to find alternatives for these murine models. A study on public attitudes toward animal testing conducted between 2014 and 2018, showed that the acceptance has slowly but steadily decreased over time (Clemence, 2018). Biomedical research for well-motivated reasons gained the highest acceptance (compared to animal usage for testing environmental chemicals and cosmetics for example). However, the study found that the "more relatable" the animal (e.g., monkey, dog, cat) and the younger the polled generation, the stronger the position against animal testing (Clemence, 2018). In this regard, improvements in the zebrafish model enabling a reduction in the usage of rats and mice, could alleviate some of the ethical stigma related to animal trials in general.

Both commercially available cell lines and PDXs have successfully been transplanted into zebrafish embryos (Hason & Bartůněk, 2019). Even though using zebrafish embryos is limited in recognizing many of the long-term changes in tumor growth, embryo xenografting has undoubtedly provided valuable information about the early features of tumor growth and metastatic cascades (Yan et al., 2019). In some cases, finding the optimal temperature for both the recipient zebrafish larvae and the transplant-specific cell type of human origin can be challenging (X. Chen et al.,

2021). In addition, the suboptimal 34 ℃ incubation temperatures typically used for xenografted zebrafish embryos, alter the proliferation rates and the histological composition of the transplants (compared to the tumors found in humans, or the engraftments performed in the murine models), something which has to be considered when interpreting results acquired from zebrafish trials (Yan et al., 2019).

The challenge of xenografts is the host systems' intrinsic tendency to tissue rejection. The zebrafish embryo lacks a functional immune system until approximately 8 days post-fertilization (Costa et al., 2020). The undeveloped adaptive immune system and the conserved signaling pathways between humans and zebrafish have made the zebrafish embryo and larvae convenient for short-term heterotopic xenografting without the need to make immune-system altering mutations or artificially downregulate immune responses before a week post-fertilization (Astell & Sieger, 2020; Costa et al., 2020; Roth et al., 2021). This is a benefit when screening for therapy responses (Fior et al., 2017). In adult zebrafish sub-lethal doses of irradiation and corticosteroid treatment can be used to inhibit the activation of immunological defense mechanisms (Hason & Bartůněk, 2019). In addition, the problem of rejection in adult fish is often tackled by making immunodeficient knock-outs/downs or administration of anti-rejection (immunosuppressant) drugs (Roth et al., 2021). Several genetically modified immunocompromised strains of fish with reduced levels of T- B- and NK cells (T- and B- lymphocytes, Natural Killer Cells) have been established and successfully used for many types of *allograft* transplantation in studies of long-term effects in adult zebrafish (Hason & Bartůněk, 2019). Until recently, the xenografting of human cells has therefore predominantly focused on embryos. The xenografting of older zebrafish has shown to be difficult and has often been limited due to the xenografts not sustaining past a week of transplantation when the developed immunity has started to reject the human cancer cells (Hason & Bartůněk, 2019). In 2019 a research group however succeeded in developing an optically clear Casper strain zebrafish deficient in *prkdc*$^{-/-}$ (Protein Kinase DNA-activated catalytic polypeptide) and *il2rga*$^{-/-}$ (Interleukin-2 Receptor Gamma a). In addition to these genetic deletions and the absence of T-cells, B-cells, and NK cells, the researchers were able to selectively breed this strain to sustain at 37℃. With this zebrafish strain, they demonstrated successful xenografting of adult zebrafish, resulting in robust tumor kinetics and histological appearance equivalent to those obtained in NSG mouse model

studies (NOD Scid Gamma, a commonly used immunocompromised strain of laboratory mice) (Yan et al., 2019).

The limitations of zebrafish embryo xenografting is the precision required to perform successful injections with minimal damage and mortality of the embryos. This could be overcome by refining the automatization of microinjecting. The yolk sac is the largest and most prominent target for early transplants. The yolk sac provides a nutritious medium rich in proteins and lipids, but not too many physical matrix structures, which might affect the tumor cell behavior (Costa et al., 2020). The zebrafish larvae establish their body plan within 2-4 dpf (days post fertilization), so this is the most favorable time window for transplants targeting a specific tissue like the perivitelline space, pericardial cavity, hindbrain ventricle, or the caudal artery in the developing embryo. A relevant advantage of PDX research in the zebrafish xenograft model, compared to the murine model, is that only small amounts of cancer cells are needed. In the future, this feature could possibly be more widely exploited for personalized cancer treatments and large-scale screening of potent drugs for a specific patient-derived biopsy specimen (Astell & Sieger, 2020). The absence of immune cells attacking the foreign cell material in embryos facilitates xenografting, but supporting xenograft survival even further with for example ECMs could be a valuable addition to the xenografting protocols.

2.5 Law and Ethics for Conducting Animal Tests on Zebrafish

Zebrafish husbandry and the use of zebrafish for research require licensing just like with any other model organisms. The regulations governing the use of animals in scientific research are established at the European Union (EU) level through Directive 2010/63/EU on the protection of animals used for scientific or educational purposes, and further supplemented by national legislation in Act 497/2013 and Decree 564/2013. These legislative measures aim to ensure the protection and welfare of animals employed for scientific or educational purposes (Finlex). The objectives of the regulations are to prioritize the utilization of alternative methods to animal testing

whenever feasible, and secondly, to minimize adverse effects on the test subjects in situations where alternatives to animal testing are not applicable.

Nevertheless, various model organisms remain an invaluable resource particularly in biomedical research as only a limited number of biological mechanisms can be fully recapitulated outside the context of a living organism. Accurate tracking and record-keeping of the number of zebrafish used for experiments is mandatory, but conducting *in vivo* experiments with embryos that do not surpass the 5-day threshold (at which point the embryo transitions into an independently feeding larvae and starts counting as a test animal), allows for a more liberal approach regarding experiments that one can conduct within this time frame at the early stages of development.

Practices regarding zebrafish husbandry differ to various extents across fish housing facilities. While this does not necessarily pose any threat to the health or well-being of the zebrafish, it might affect the results obtained in trials conducted at different laboratories (Aleström et al., 2020). For this reason, reporting details of the husbandry practices in any conducted study has become a more widespread practice. Another approach to solving the variability issue is the collaboration effort made between the European Society for Fish Models in Biology, and the Federation of European Laboratory Animal Science Association (FELASA). This work aims to establish comprehensive guidelines for the standardization of crucial elements in zebrafish husbandry practices, such as protocols for quarantine practices for laboratories receiving new fish strains, facility hygiene requirements, water temperature and quality monitoring, dark-light cycle standardization, fish density and space requirements, as well as specifications for feeding practices and breeding procedures (Aleström et al., 2020). These initiatives are indeed welcomed, as they further strengthen the rigorousness and reproducibility of zebrafish-related research outcomes.

3 Aims of the Study

This master's thesis project investigates the potential to use various extracellular matrix components, commonly utilized to optimize *in vitro* cell cultures, as xenograft supports in the zebrafish cancer model. The selected matrixes for this project include Grow-Dex®, Matrigel®, PureCol® (collagen), Fibronectin, and Gelatin.

The study begins with assessing the general suitability of viscous matrixes in conjunction with the Nanoject II microinjector equipment. The viscous matrixes may alter the xenograft media, making it more challenging to inject into zebrafish embryos. This issue is expected to be overcome by adequately diluting the matrixes, while the matrix would still provide growth benefits to the xenograft compared to the commonly used xenograft medium PBS (Phosphate-Buffered Saline). The imaging data of the fluorescently labeled xenografts will be analyzed to evaluate the ECM's effect on the transplanted MDA-MB-231 mCherry tumor cells.

In zebrafish, tumor xenografts are typically labeled with a fluorescent marker, and the tumor size measured by fluorescent imaging. This method has its limitations, whereby finding and standardizing a gene sequence abundant and reliable enough for qPCR and MDA-MB-231mCherry tumor cell detection from zebrafish embryos would bring more accuracy and exactness to the procedure of quantifying the tumors. The interchangeability of the two detection methods, imaging protocols and qPCR, is assessed to determine their reliability in producing comparable results.

Objectives

- To evaluate the micro-injectability of extracellular matrixes for zebrafish xenografting
- To evaluate the effects of the ECMs (tumor "take," growth, and dissemination rates) on transplants using fluorescent imaging and image analysis
- Examine qPCR as an alternative for MDA-MB-231 mCherry tumor cell detection from zebrafish embryos, to improve tumor quantification methods in the zebrafish xenograft model

4 Materials and Methods

4.1 Licensing for Zebrafish Experiments

The zebrafish embryo experiments were conducted in accordance with the Act on the Protection of Animals Used for Scientific or Educational Purposes (497/2013) and the Government Decree on the Protection of Animals Used for Scientific Purposes (564/2013), under the license number ESAVI/31414/2020. All experiments took place at the premises of the Zebrafish Core Facility at Turku Bioscience Center/ UTU/ ÅAU, Turku, Finland.

4.2 Zebrafish Embryo Culture

The Casper-strain zebrafish used for breeding the embryos were kept in a laboratory fish multi-rack system, at 28.5 ℃ and fed standard fish feed in accordance with guidelines presented in The Zebrafish Book; A guide for the laboratory use of zebrafish (*Danio rerio*) by M. Westfield 2000.

A mating tank with a suitable perforated shallow bottom was prepared with 28.5 ℃ tank water and pebbles to mimic natural habitats to encourage egg-laying. For fluorescent imaging, the strain of un-pigmented opaque Casper strain zebrafish was used. The Casper zebrafish is a result of crossing two mutant strains with defects in the main pigment genes (Figure 3). The Nacre strain lacks a functional gene for melanocytes (dark pigment), while the Roy Orbison strain lacks the functional gene for iridocytes (the light-reflecting pearly silverish pigment typical for fish) (Figure 3). Although the Casper strain has a defect in the main genes coding for dark pigmentation, they typically develop pigmentation in the structures of the eye. PTU (Phenylthiourea) is a reversible antagonist of tyrosinase, a key enzyme participating in the melanogenic pathway, therefore commonly used to inhibit the formation of dark pigmentation in many different model organisms (Li et al., 2012). In addition to the inhibition of melanization, PTU has also been shown to interfere with the development

of the eye structures, resulting in smaller eyes with decreased sizes of the retina and the lens (Li et al., 2012). This effect is presumably mediated through one or several alternative pathways separate from melanization, one of the suggested ones being PTUs' ability to inhibit TPO (Thyroid Peroxidase), leading to delayed eye development (Li et al., 2012). However, the addition of PTU (see Appendix I) in the incubation media of the embryos, has dual inhibitory effects on both eye structure development and pigment formation and was therefore utilized to ensure a clearer fluorescent signal from the head area.

Zebrafish males and females (3 of each in every tank) were collected from the maintenance tank with a fishnet and transferred to the pre-prepared mating tanks. Different strains have some specific but very subtle color differences; hence the male and female are most easily distinguished by the form of their belly. The female has a rounded belly, and in the Casper strain, the eggs are almost visible through the skin. The male is more streamlined, and in the Casper strain slightly more yellowish at the tail and fins. The mating tank was left overnight, and the eggs harvested the following morning. For experiments requiring a larger number of embryos, or synchronized embryos in the same developmental stage, the fish can be placed in the same tank overnight separated by a wall. Being in the same tank, but not removing the wall until the morning, can enhance egg laying, and ensure that most of the eggs are fertilized in a narrower time window.

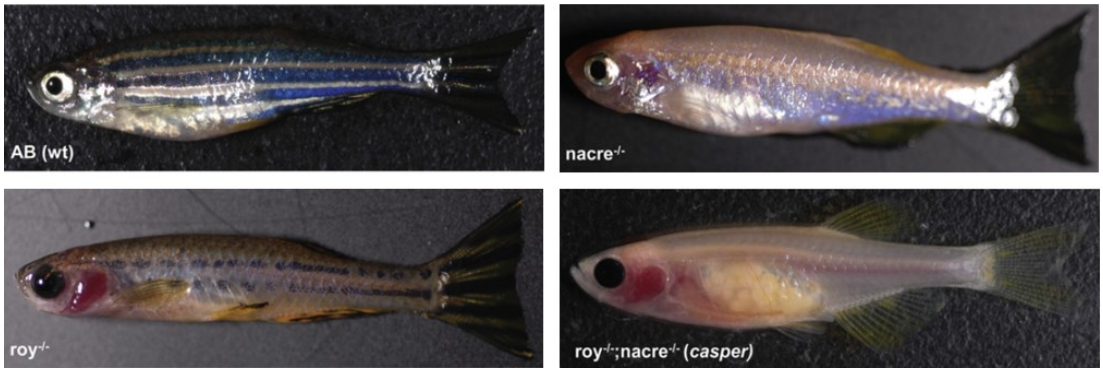

Figure 3: Zebrafish strains. AB wildtype (top left) has normal melanocyte and iridocyte expression and the typical appearance of a striped zebrafish. Nacre strain fish (top right) have the normal genes for iridocytes (the pearly silver color) but are recessive homozygotes for a mutated melanocyte pigment gene. The Roy Orbison strain (lower left) has normal melanocytes but lacks iridocytes (also making the bluish color of the melanocytes look dim). The Casper strain (lower right) lacks both pigment genes, making them opaque and almost see-through. (Picture used with permission of White et al., 2008).

The adult zebrafish were removed from the mating tank, and the eggs collected from the bottom of the tank by pouring the water through a strainer. Fish debris was removed from the embryos by gently washing the eggs with tank water, after which the eggs were transferred into Petri dishes by gently pouring water through the upside-down strainer.

The timeline for producing zebrafish embryos for xenografting is presented in Figure 4. The collected fish eggs were examined under a stereomicroscope and unfertilized or malformed eggs discarded. Approximately 50 healthy-looking eggs per dish were transferred into 10cm Petri dishes with fresh E3+PTU-media (see Appendix I) by pipetting. The embryos were incubated at 28 °C for 48 hours at which point most of the eggs would have hatched spontaneously, but to ensure effective hatching, Pronase® enzyme 20mg/ml was added (20 µl per 20 ml Petri dish) at 24 hours post fertilization. Pronase® is a commercially available mixture of proteases (neutral proteases, chymotrypsin, trypsin, carboxypeptidase, aminopeptidase, and neutral and alkaline phosphatases) isolated from *Streptomyces griseus*, which effectively weakens the egg wall. Any unhatched eggs were dechorionated by hand with forceps and by gently pipetting the eggs up and down a few times. Microinjections were performed 2 days (~48h) post-fertilization.

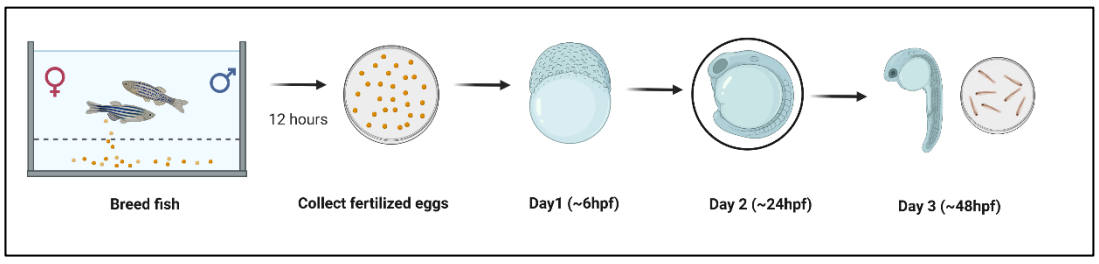

Figure 4: Zebrafish mating setup. Zebrafish males and females are put in a mating tank. Mating occurs in the morning hours when the laboratory lights (simulating sunrise) turn on. At approximately 6 hpf (hours post fertilization) the successfully fertilized eggs are distinguishable due to the blastoderm (~1000+ cell stage), a cell mass formation before the egg undergoes epiboly, and the cells start to migrate around the edge of the yolk sac. Eggs are collected and incubated at 28 °C for 48 hours, at which point embryos have hatched from the egg sacks. Zebrafish embryos are ready for xenografting 2 dpf (days post-fertilization). (Figure created with Bio Render).

4.3 Preparation of ECMs and Nanoject II calibration

ECMs, which are viscous and sticky, can be challenging to work with even in normal cell culturing performed in dishes and flasks. For the Nanoject II apparatus 3,5" Drummond# 3-000-203-G/X capillary needles were pulled with a GWB Narishige Japan PB-7 needle puller. To measure the extent to which the addition of viscous matrixes causes needle blockages or alterations to the droplet volumes ejected by the Nanoject II microinjector, a dilution series of each ECM-media was done and compared to PBS that is typically used as xenograft media (Figure 5). Ideally, the ECMs would not affect the volume of solution ejected by the microinjector. The ECM solutions were later to be mixed with cancer cells to contain a final concentration of $10x10^7$cells/ml, further adding to the viscosity of the liquid needing to pass through the capillary needle.

The ECMs tested in this project were Grow-Dex®, Matrigel®, PureCol® (collagen), Fibronectin, and Gelatin (see Appendix I). To establish a directive for what concentration of each ECM could be used with the microinjector, a dilution series, six concentrations for each ECM, was made by mixing 1:1 of descending concentrations (Table 1). ECM stock was mixed with an equal amount of media (PBS for Grow-Dex®, PureCol®, and Gelatin, DMEM for Matrigel®, and milli-qH_2O for Fibronectin). To facilitate the observation of the backfilling of the capillary needle when microinjecting, and to indicate pH when diluting the PureCol® that needs to be neutralized with 0.1M NaOH to activate collagen fiber-formation, 5µl 0.5% phenol red was added to each ECM-mix.

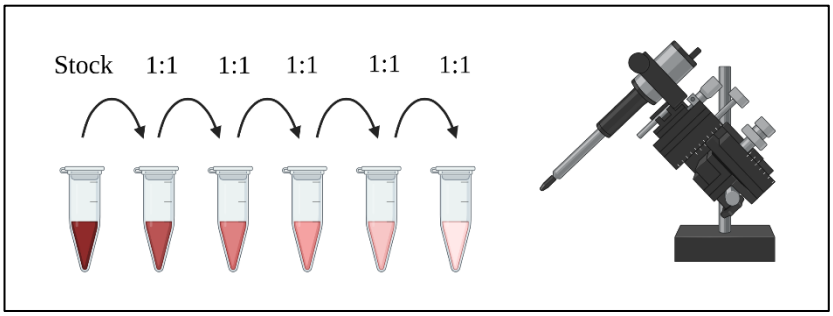

Figure 5: Crude dilutions for establishing what concentrations of ECM could be used with the tumor cell solution to be injected with the Nanoject II equipment. (Figure created with Bio Render)

Table 1: Dilution series made from the ECM stock solutions, six concentrations each. The calibration started with the mildest concentration, working the way up to determine if needle blockage would become a restrictive factor.

Dilution	Grow-Dex® 1.5%	Matrigel® 19.8mg/ml	PureCol® 2,9mg/ml	Fibronectin 1mg/ml	Gelatin 10%
1.	0.75%	9.8mg/ml	0.232%	5µl/ml	1%
2.	0.375%	4.9mg/ml	0.116%	2.5µl/ml	0.5%
3.	0.1875%	2.45mg/ml	0.058%	1.25µl/ml	0.25%
4.	0.09375%	1.225mg/ml	0.029%	0.75µl/ml	0.125%
5.	0.046875%	0.6125 mg/ml	0.0145%	0.375µl/ml	0.0625%
6.	0.0234375%	0.30625 mg/ml	0.00725%	0.1875µl/ml	0.03125%

The ECMs that require handling in cool temperatures (Matrigel®, PureCol®, and Fibronectin) were held on ice and kept cool during the preparation. All dilution media (PBS, DMEM, and milli-qH_2O) were likewise kept on ice and mixed in pre-cooled vials with pre-cooled pipette tips. This was done to prevent the ECMs from starting to solidify before the procedure of injecting submerged droplets into the calibration oil.

The capillary needle was pre-filled with mineral oil (see Appendix I) and backfilled with ECM solution by aspirating the solution into the Nanoject II microinjector apparatus. ECM droplets were injected into Halocarbon 27 oil, a commonly used oil for microinjector calibrations. To test the consistency of the droplets for all matrixes, the microinjector was installed to administer 13.8 nL (fast speed). This was the minimum droplet size needed to overcome the hydrophobic properties of the Halocarbon 27 oil. Too minuscule volumes/ light droplets, even when ejected in a uniform manner, tended to stick to the capillary needle tip and rise to the surface, rather than remain under the surface for accurate measurements. The smaller volumes (4.6 nL) planned to be injected into the zebrafish embryo were not expected to face the same problem since the yolk sac membrane and the aqueous surrounding in the yolk sac would prevent the tumor-ECM droplet from following the needle tip as it did in the oil environment. After photographing the droplets with a Hamamatsu sCMOS Orca Flash 4.0 LT+, using a Zeiss Axxio Zoom V16 microscope, the droplet diameter was measured using Fiji ImageJ analyzing software for volume calculations.

4.4 Cell Culture

4.4.1 MDA-MB-231 mCherry, Human breast carcinoma cells

MDA-MB-231 is an immortalized human-derived cell line commonly used in cancer research. It was initially isolated at M.D. Anderson Hospital and Cancer Research Center in Houston, Texas, USA. The cell line originates from a woman with reoccurring breast cancer (MDA= abbreviation of the hospital, MB= Metastatic Breast (cancer)). Later, different variants of the cell line have been generated through repeated passaging *in vitro* of metastases isolated from either the bone or the brain of nude mice (Welsh, 2013). These MDA-231BO (bone-seeking) and MDA-231BR (brain-seeking) cell lines have shown a preference for migrating to their specific tissues of isolation. This has aided researchers in studying the features of cancer cells in conjunction with the tumor microenvironment that affects the tendency of a particular tumor cell to navigate to a specific metastatic niche (Welsh, 2013). Furthermore, commercially available widely used strains of MDA-MB-231 have been incorporated with genes producing luciferase, GFP (Green Fluorescent Protein), or mCherry, emitting red fluorescence. These fluorescent markers enable convenient tracking of the growth, location, and migration of tumor cells both *in vitro* and *in vivo*.

MDA-MB-231 is, by definition, a tumor cell line of invasive ductal epithelial carcinoma (adenocarcinoma) that exhibits traits indicating a highly treatment-resistant variant of breast cancer known as TNBC (Triple-Negative Breast Cancer) (Huang et al., 2020). It lacks the typical over-expression of all the three main receptor types known to fuel breast cancer growth and that are common targets in breast cancer treatment: ER (Estrogen Receptor), PR (Progesterone Receptor), and Her2 (Human Epithelial growth factor 2 Receptor). The downregulation of E-cadherin expression (an important adhesion protein maintaining cell-cell contact and an important marker associated with “stationary” cells), and the presence of a mutated p53 tumor-suppressor (hence instead accelerating tumor progression), results in a highly proliferative and migratory phenotype of tumor cells (Welsh, 2013).

The properties of MDA-MB-231 mCherry, being durable and prone to EMT and metastases, combined with being fluorescently labeled, made it especially suitable for our specific purposes of cross-species xenografting and *in vivo* imaging. Secondly, past experience of MDA-MB-231 enduring several types of xenografting (Benton et al., 2011; Maity et al., 2011; Yoshida, 2020) confirmed the decision to use this strain as a starting point for trying out modifications to the xenografting routines. If the alterations to the zebrafish embryo xenograft protocol turned out to be beneficial, the method could later be applied to other more sensitive cell lines.

Passage 3 MDA-MB-231 mCherry cells (see Appendix I) were thawed from liquid nitrogen in RT (room temperature). To establish a stable cell culture, the cells were grown and left to recover on 100 mm culture dishes in DMEM+glucose media fortified with 10% Fetal Bovine Serum, 1% glutamine, and 1% Penicillin-Streptomycin mix (see Appendix I) and incubated at 37 ℃ under 5% CO_2 for four days.

The cells were provided with fresh media and split every ~3-4 days to prevent overgrowth. This was done by removing the growth media and washing the cells with 5ml PBS. After the PBS was removed, 1.8ml PBS and 200µl 10x Trypsin-EDTA solution was added to start the enzymatic breakdown of the proteins attaching the cells to the growth plate. The cells were incubated for 3-5 minutes at 37 ℃ and checked every few minutes under the microscope, to monitor the degree of cell dissolvement. These cells multiply rapidly, resulting in high concentrations of tumor cells; therefore, 200µl cell suspension per 100mm dish in 10ml DMEM-media was used at every passage and plate splitting (Figure 6).

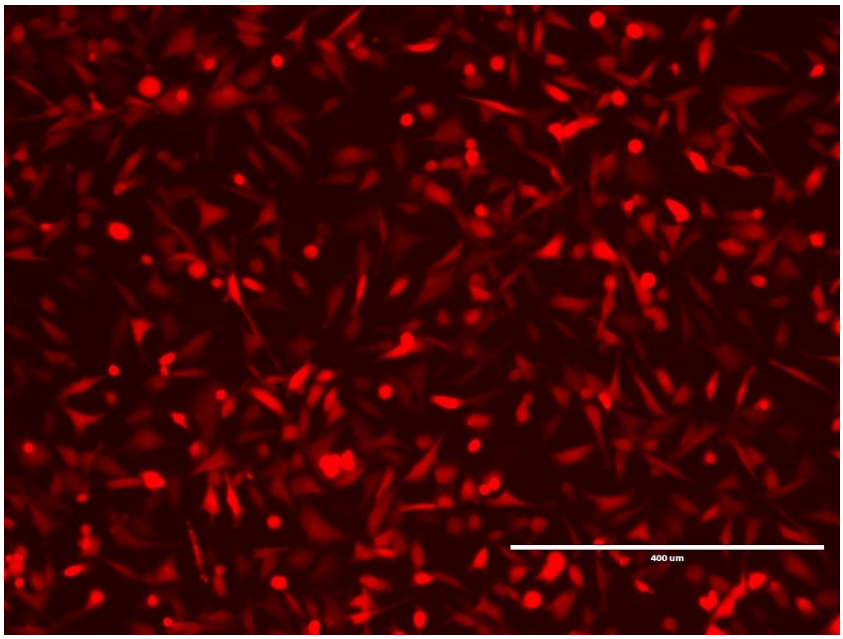

Figure 6: Confluence of MDA-MB-231 mCherry cell culture under red fluorescence before plate splitting. (Photograph by ©Nina Ylinen).

4.4.2 MDA-MB-231 mCherry cell extracts

The cells were dissolved from the cell culture dish by removing the growth media, washing with 5ml PBS, adding 2ml PBS + 0.05% trypsin-EDTA solution, and incubating the plates for 6 minutes at 37 ℃. The cell solution was pipetted into 15ml falcon tubes with 5ml DMEM media to neutralize the enzymatic breakdown of proteins. The tubes were centrifuged at 200g for 4 minutes, the supernatant aspirated, and the cell pellet resuspended in 1 ml PBS for concentration measurements using the automated Innovatis Cedex3271 XS cell counting device and software. The equivalent of 1 million cells was transferred into Eppendorf tubes, the Eppendorf's centrifuged at 200g for 4 minutes, the supernatant removed, and the ~1 million cells per pellet used for DNA extraction.

4.4.3 qPCR and standard curves for MDA-MB-231 mCherry detection

qPCR (Quantitative Polymerase Chain Reaction) is a nucleic acid amplification method used to measure the amount of a specific gene product as it is replicated in real time (Figure 7). Once the product of interest is amplified beyond a specific Ct-value (cycle threshold value), the fluorescent marker emits a signal correlating to the amount of the gene product present in the sample. qPCR is an extremely sensitive method for detecting small amounts of gene product when correctly tuned. However, optimizing the starting concentrations and not exceeding amplification cycles is crucial for avoiding unspecific primer and amplicon binding that can generate noisy results.

To assess for a gene sequence that could be utilized for MDA-MB-231 mCherry xenograft detection, qPCR kit PowerUp™ SYBR™ Green Master Mix and two different sets of primers were used. The zebrafish xenograft was planned to be 4.6nL, meaning only some hundred tumor cells would be transplanted in each embryo. Therefore, the aim was to find a gene and a range within which the qPCR could be performed, sensitive enough to recognize even minute amounts of human DNA present in the single zebrafish embryo sample. The two gene sequences of choice landed on one human-specific nuclear gene sequence and one human-specific mitochondrial DNA sequence, with the mitochondrial DNA expected to be more abundant in especially rapidly dividing MDA-MB-231 mCherry cells.

The DNA from the MDA-MB-231 mCherry cancer cell pellets (prepared in section 4.4.2) was extracted using a modified version of the Hot-Shot protocol. The same protocol would later be used when extracting whole DNA from the single embryo samples. The pellet consisting of 1 million MDA-MB-231 mCherry cells was dissolved in 180µl NaOH and heated at 95 ℃ for 10 minutes while vortexing every 3 minutes to ensure complete dissolvement of the membrane structures. The cell solution was cooled down, neutralized with 20µl Tris-HCL, and the cell debris spun down for the DNA-containing supernatant to be used for the qPCR reaction.

A dilution series of the 5000cells/µl DNA extract was made by taking 10µl of the stock DNA extract+90µl milli-qH_2O and diluting down 1:10, resulting in concentrations of 500, 50, 5, 0.5, and 0.05 cells/µl. Using 2µl of these dilutions for the qPCR reaction would approximate the cycle thresholds needed to detect 10 000, 1000, 100, 10, 1, and 0.1 tumor cells present in the sample.

The qPCR runs were carried out by TaqMan plate running service (Finnish Functional Genomics Center Core Facility, Bioscience Center, Turku, Finland), using QuantStudio™ 12K Flex Real-Time PCR System (Thermo Fisher Scientific). The collected data was further analyzed with RQ software in the Thermo Fisher cloud service.

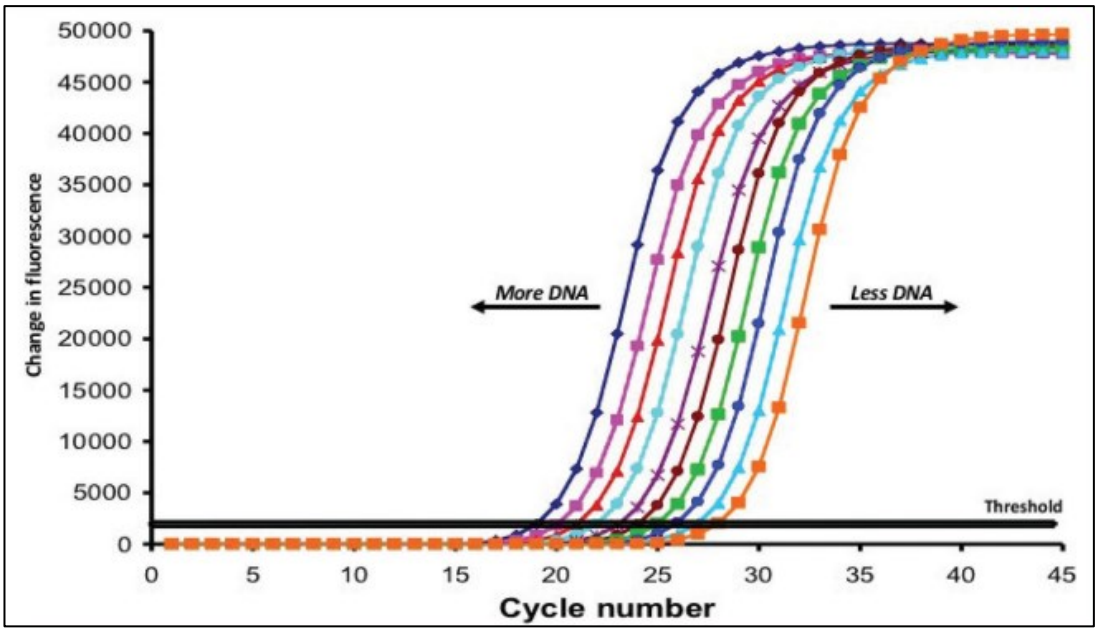

Figure 7: The principle of gene detection with qPCR. Every thermal cycle amplifies the signal originating from a specific gene sequence twofold from the amount present at the previous cycle. The more target gene present at the beginning of the reaction, the fewer amplification cycles needed before a fluorescent signal can be detected. (The Figure used with permission of Severine Tasker et al. 2018).

4.5 Tumor xenografting with ECMs

4.5.1 Preparing ECM & MDA-MB-231 mCherry xenografts

Due to the difficulties of handling and achieving homogenous suspensions of the Grow-Dex® matrix in small volumes, the decision was made not to use it for the actual xenograft experiments. The ECM concentrations for Matrigel®, PureCol®, Fibronectin, and Gelatin were chosen in accordance with the most concentrated solution still effortlessly injectable with the Nanoject II microinjector during the calibration experiment (Matrigel® 9,8%, PureCol® 0,232%, Fibronectin 5µl/ml, and Gelatin 1%).

Matrigel® stock solution (see Appendix I) was thawed on ice in the refrigerator overnight and diluted with ice-cold DMEM media to a final concentration of 9.8%. The mixing was performed on ice, using all pre-cooled vials and pipetting equipment to prevent the gelling reaction from starting. PureCol® (see Appendix I) collagen was prepared according to the manufacturer's instructions for 3D gel preparation to 0.232%, by taking eight parts chilled PureCol® and 1-part chilled PBS and adding 5µl phenyl red. To activate the collagen polymerization reaction, the pH was adjusted from acidic to a neutral 7-7.5 with 0.1M NaOH using the color of phenyl red as the pH indicator. Finally, the volume was adjusted to a total of ten parts with more ice-cold PBS. All vials, tubes, and pipettes were kept on ice during the preparation procedure to prevent polymerization which for PureCol® peaks at 37°C. The 1mg/ml Fibronectin stock solution (see Appendix I) was thawed overnight, and the concentration recommended for cell culturing (5 µl/ml) was made by diluting it with ice-cold milli-Q water. Like Matrigel® and PureCol®, Fibronectin also starts gelling at room temperature, so the vials were kept on ice, and excess agitation avoided.

The Gelatin 1% remaining in a liquid state at room temperature, was diluted 1:10 from a pre-made solidified 10% stock (see Appendix I). The stock solution was heated to boiling point by microwaving and then mixed with 9 parts PBS in RT.

A cell solution of $10x10^7$cells/ml of MDA-MB-231 mCherry was made for the purpose of injecting 4.6 nL as zebrafish embryo xenografts. The cell plates were washed with 5ml PBS, trypsinated from the culture plates, and the cell solution neutralized with DMEM-media. After concentration measurements, 1 ml of cell solution was transferred into Eppendorf tubes. The Eppendorf tubes were centrifuged at 200g for 8 minutes and the supernatant removed, obtaining a cell pellet with a known cell count. The cell pellet was then resuspended with the different ECM solutions to a final concentration of one hundred million cells per milliliter (Figure 8).

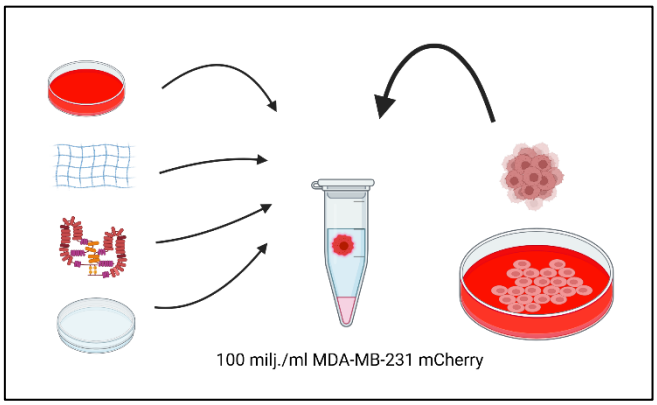

Figure 8: The highest concentration injectable with Nanoject II microinjector was chosen for each ECM. The ECM stock was added to the cell pellet to obtain a xenograft solution with 100milj/ml concentration of MDA-MB-231 mCherry. (Figure created with BioRender).

4.5.2 Xenografting and Visualizing Tumor Survival and Growth

The fluorescently labeled cancer cells' relative amount (and location) can easily be detected in the transparent zebrafish embryo by fluorescent microscopy (Figures 9A and 9B). Xenograft transplants of MDA-MB-231 mCherry into zebrafish were performed 48h post-fertilization. Fertilized eggs were collected and transferred into Petri dishes according to the protocol presented in 4.2. After 48 hours of incubation at 28 °C the embryos were sedated in ~200mg/ml Tricaine bath, by adding 1ml MSM222 stock-solution (4g/l) to crudely 20 ml E3+PTU media in each Petri dish.

The workflow of xenografting and visualization of zebrafish embryos is presented in Figure 9B. The sedated zebrafish larvae were transferred in anesthesia media and mounted on agarose comb plates made from 2.5% Agarose in milliQ-H_2O. The wells/rows keep the larvae stationary underwater for the injection procedure (Figure 9B). The agarose was heated and melted in the microwave oven, poured on a Petri dish lid (for lower edges facilitating microinjections), a plastic mold placed on the surface of the agarose, and left to solidify for approximately 1 hour. Once organized in the comb rows, the embryos were injected (in the yolk sac) with 4.6 nL of 100milj/ml MDA-MB-231 mCherry in the different ECM-fortified media. The injected larvae (approximately 50 larvae per test group) were collected from the comb plates and transferred into Petri dishes with fresh E3+PTU media. As a compromise temperature suitable for both zebrafish embryos and human cancer cells, the embryos were subsequently incubated at 34 ℃. This temperature setting, although not perfectly optimal for either zebrafish embryos or human tumor cells, does meet the requirements of both biological systems to sustain.

One day post injection (dpi), the embryos were sedated (Figure 9A), and successfully xenografted embryos chosen to be transferred from the Petri dish into 24-well plates, one embryo in each well. The embryos were visualized at two time points, 1dpi and 4dpi, using Axio Zoom wide-field fluorescent microscope and Hamamatsu camera. Each well was imaged with two channels, brightfield, and Texas Red with Alexa fluor 555. The emitted fluorescence and its intensity translating into cell survival and tumor growth rates were measured using FIJI software and ImageJ analyzing tools. The results of fluorescent intensity at 4dpi were in addition later compared to the quantities of tumor cells detected by qPCR.

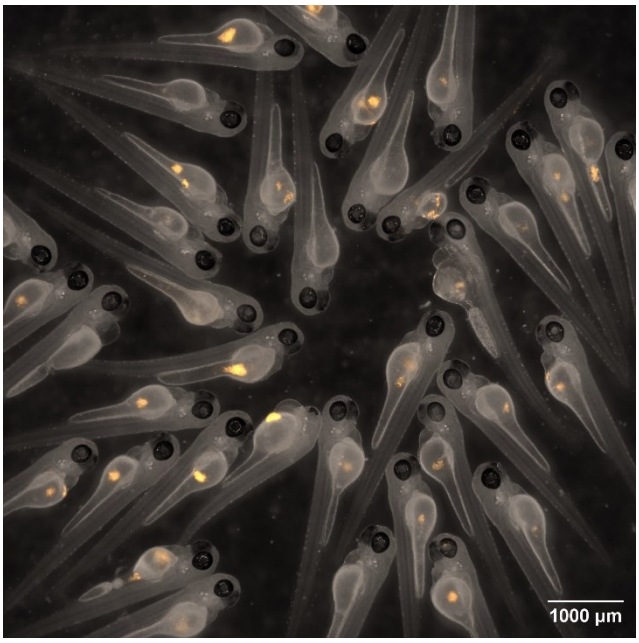

Figure 9A: Zebrafish embryos imaged 1 day after being injected with fluorescent MDA-MB-231 mCherry breast cancer cells. The xenograft was planted in the yolk sac of the embryo (© Photograph by Nina Ylinen).

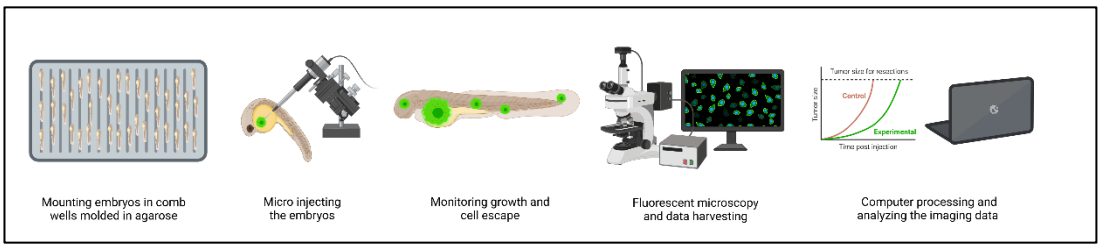

Figure 9B. Workflow for zebrafish xenograft detection by microscopy. The sedated embryos were mounted in anesthesia medium in organized rows, where the wells on the agarose mold in the bottom of the Petri dish kept the embryos in place. The tumor cells were injected into the yolk sac of the embryo under the microscope. The cancer cells' survival rate, growth, and migration were visualized with fluorescent imaging methods, and the intensity analyzed with Fiji ImageJ software. (Figure created with Bio Render).

4.5.3. qPCR and Hot-Shot protocol for DNA extraction

The quantity of MDA-MB-231 mCherry cancer cells of human origin in the zebrafish embryo was assessed with real-time qPCR for correlative comparison with the results from the image analysis data taken 4 days post-injection (Figures 10A and 10B). Following the imaging, each labeled embryo was transferred into an Eppendorf tube, and excess water carefully removed. To dissolve the embryo and the cell membranes, 50 µl of 50mM NaOH was added, and the tubes heated at 95 ℃ for 20 minutes. The tubes were vortexed every ~5 minutes to ensure complete dissolvement. The tubes were cooled down on ice, and 5.5 µl of 1M Tris-HCl (pH 8) added to neutralize the NaOH. The tubes were finally centrifuged at top speed for 5 minutes to spin down unwanted cell debris, and the supernatant used for the qPCR protocol.

The qPCR was done using PowerUp™ SYBR™ Green Master Mix from Applied Biosystems (see Appendix I). The Master Mix was prepared with the forward and reverse primers (see Appendix I) for the human mitochondrial DNA, which showed higher sensitivity in the previously performed standardization tests. The reactions were made as triplicates of each sample in a 96-well plate, as 10µl reactions (8µl Master mix + 2 µl DNA extract). Triplicates of purified H_2O and embryo DNA extract without xenograft transplant were used as negative controls. The qPCR runs were carried out by TaqMan plate running service according to the standard run files provided, with QuantStudio™ 12K Flex equipment. The reaction was initiated with 2min 95 ℃ (ramping heat by 2.63 ℃/second) to activate the DNA polymerase. This was followed by 40 cycles of 15 seconds of denaturation at 95 ℃ (ramping heat by 2.63 ℃/second) and annealing for 2 minutes at 60 ℃ (heat reduction by 2.42 ℃/second) and the sample fluorescence recorded after each cycle. The reaction was completed with the melt curve analysis; heating the samples for 15 seconds to 95 ℃ for denaturation (ramping heat by 2.63 ℃/second), lowering the temperature to 60 ℃ for 1 minute (2.42 ℃/second) for the strands to anneal, and finally denature the strands at a slow speed (0.5 ℃/second) to 95 ℃ for 15 seconds. This was to confirm the specificity of the qPCR products and exclude the possibility that signals obtained at the cycling phase would originate from unspecific amplicon products.

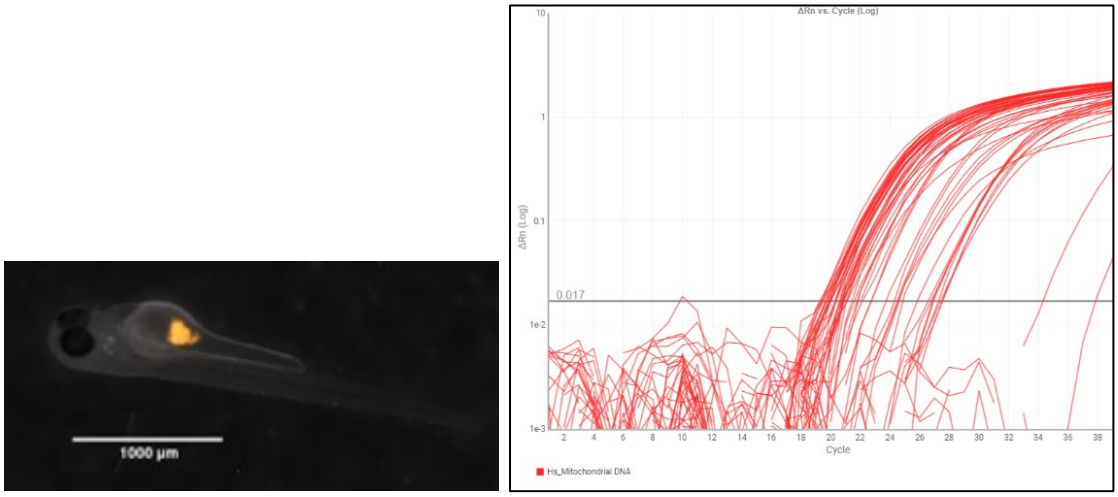

A) B)

Figure 10: **A)** The zebrafish embryos were imaged 4 days post-injection for fluorescent intensity analysis, after which the DNA was extracted from each labeled embryo. **B)** The fluorescent intensity was compared to the cycle threshold values of rt-qPCR, detecting human-specific mitochondrial DNA, to see how well the two tumor detection methods would correlate.

4.6 Statistical Analyses

Statistical analyses were done with SPSS software, version 29.0, using Kruskal-Wallis and Mann-Whitney tests. The qPCR data and the results obtained by visualizations and Fiji software analyses for fluorescence intensity were analyzed to determine the extent of correlation between the two measurement methods. The fluorescence of tumors transplanted in the different ECM mediums was compared with each other using Kruskal-Wallis's statistical analyses examining if any meaningful variation in the success rate of xenografts, or differences in growth rates, was to be found between the two time points of imaging. The reduction of variability between the different groups was compared by Kolmogorov-Smirnov type II tests.

5 Results

5.1 Extracellular matrixes are compatible with Nanoject II

The droplet volumes of the matrix solutions (Grow-Dex®, Matrigel®, PureCol®, Fibronectin, and Gelatin) at different concentrations injected in HaloCarbon27 oil, are presented in Figures 11-15. To get measurable droplets in the hydrophobic calibration oil, the microinjector was set to administer 13,8nL. The major challenge for the overall usage of the ECMs with the microinjector was not needle blockages as anticipated, but the difficulties of accurate calibration caused by surface tensions and adhesive forces between the droplet and the capillary needle.

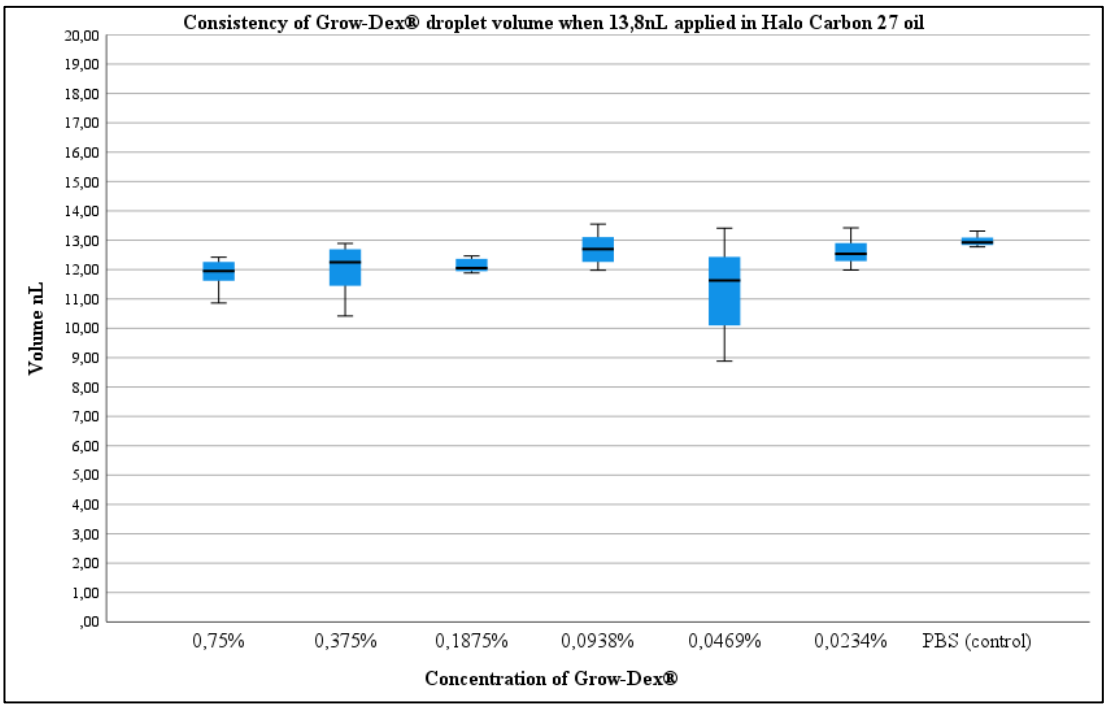

Figure 11: Variation in calculated droplet volumes with decreasing concentration of Grow-Dex® compared to the PBS control *(M* = 12.96, *SD* = 0.19*)*: Grow-Dex® 0.75% (*M* = 11.84, *SD* = 0.557), 0.375% (*M* = 11.99, *SD* = 0.93), 0.1875% (*M* = 12.13, *SD* = 0.23), 0.0938% (*M* = 12.71, *SD* = 0.60), 0.0469% (*M* = 11.35, *SD* = 1.70), and 0.234% (*M* = 12.61, *SD* = 0.50).

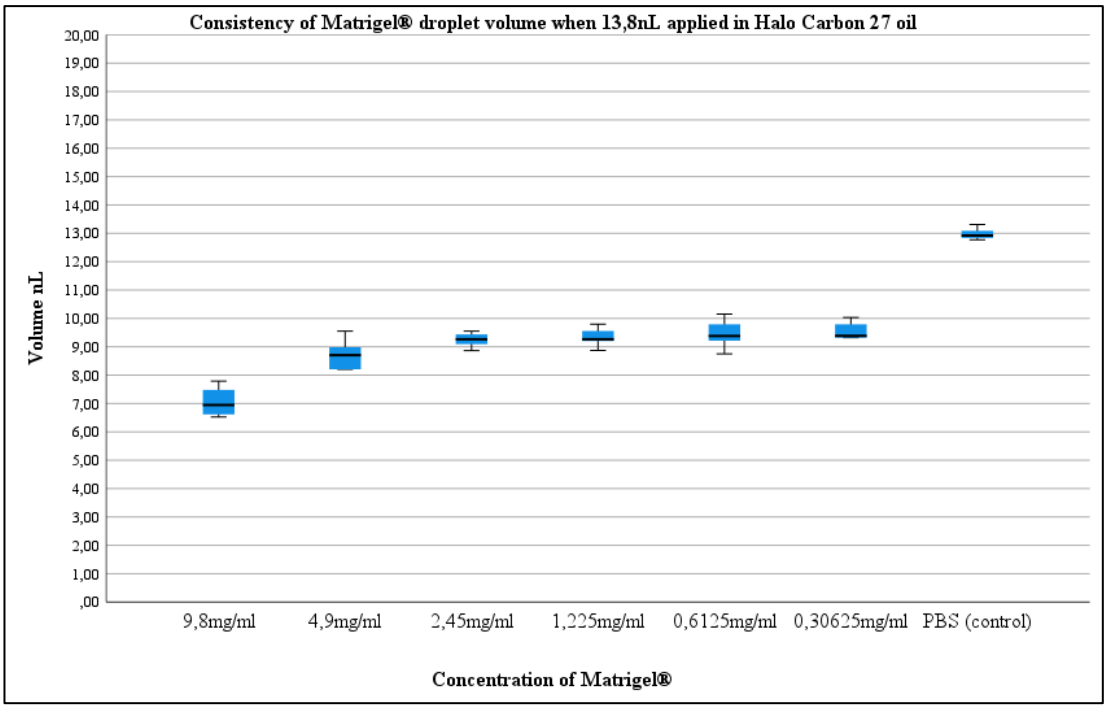

Figure 12: Variation in calculated droplet volumes with decreasing concentration of Matrigel® compared to the PBS control *(M* = 12.96*, SD* = 0.19*)*: Matrigel® 9.8mg/ml (*M* = 7.05, *DS* = 0.52), 4.9mg/ml (*M* = 8.72, *SD* = 0.51), 2.45mg/ml (*M* = 9.24, *SD* = 0.27), 1.225mg/ml (*M* = 9.325, *SD* = 0.32), 0.61255mg/ml (*M* = 9.44, *SD* = 0.48), and 0.30625mg/ml (*M* = 9.54, *SD* = 0.30).

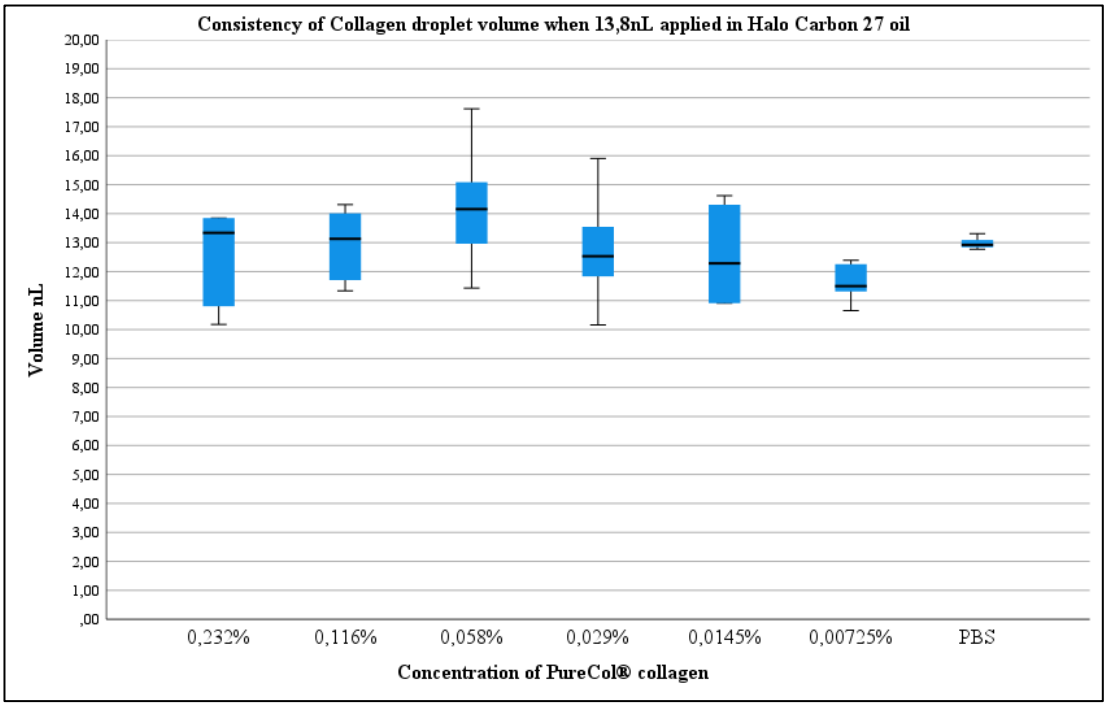

Figure 13: Variation in calculated droplet volumes with decreasing concentration of PureCol® compared to the PBS control (*M* = 12.96, *SD* = 0.19): PureCol® 0.232% (*M* = 12.56, *SD* = 1.63), 0.116% (*M* = 12.94, *SD* = 1.32), 0.058% (*M* = 14.24, *SD* = 2.10), 0.029% (*M* = 12.75, *SD* = 1.91), 0.0145% (*M* = 12.55, *SD* = 1.71) and 0.00725% (*M* = 11.60, *SD* = 0.64).

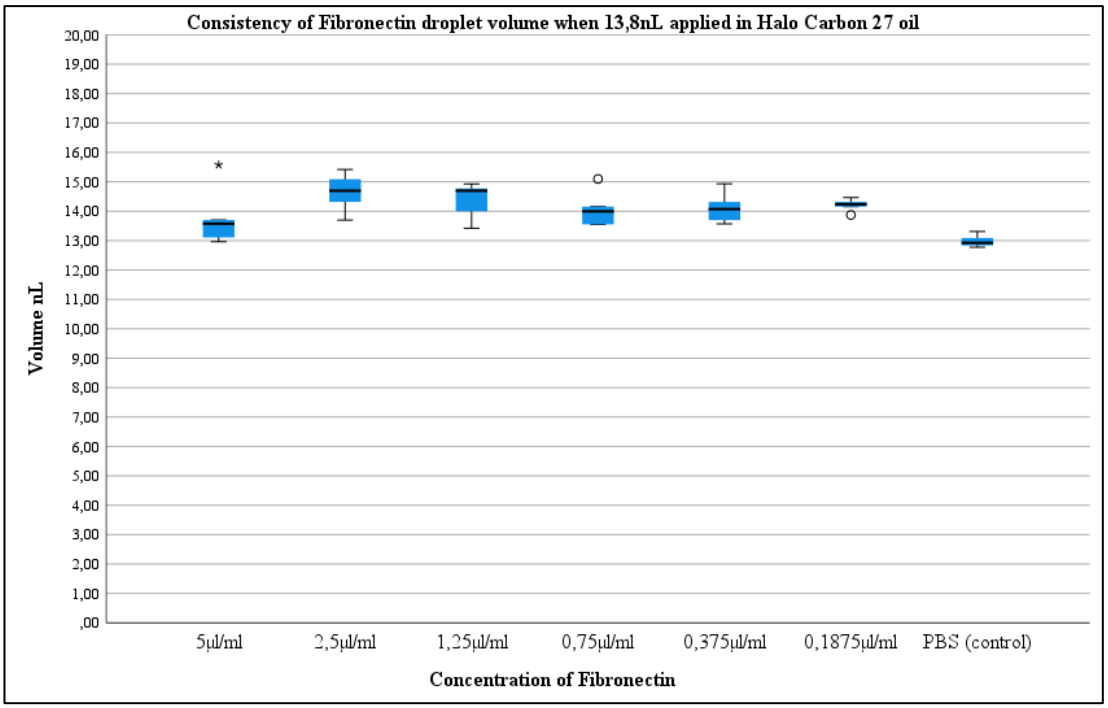

Figure 14: Variation in calculated droplet volumes with decreasing concentration of Fibronectin compared to the PBS control (*M* = 12.96, *SD* = 0.19): Fibronectin 5 µl/ml (*M* = 13.74, *SD* = 0.94), 2.5 µl/ml (*M* = 14.5, *SD* = 0.60), 1.25 µl/ml (*M* = 14.42, *SD* = 0.59), 0.75 µl/ml (*M* = 14.06, *SD* = 0.57), 0.375 µl/ml (*M* = 14.11, *SD* = 0.49) and 0.1875 µl/ml (*M* = 14.21, *SD* = 0.20).

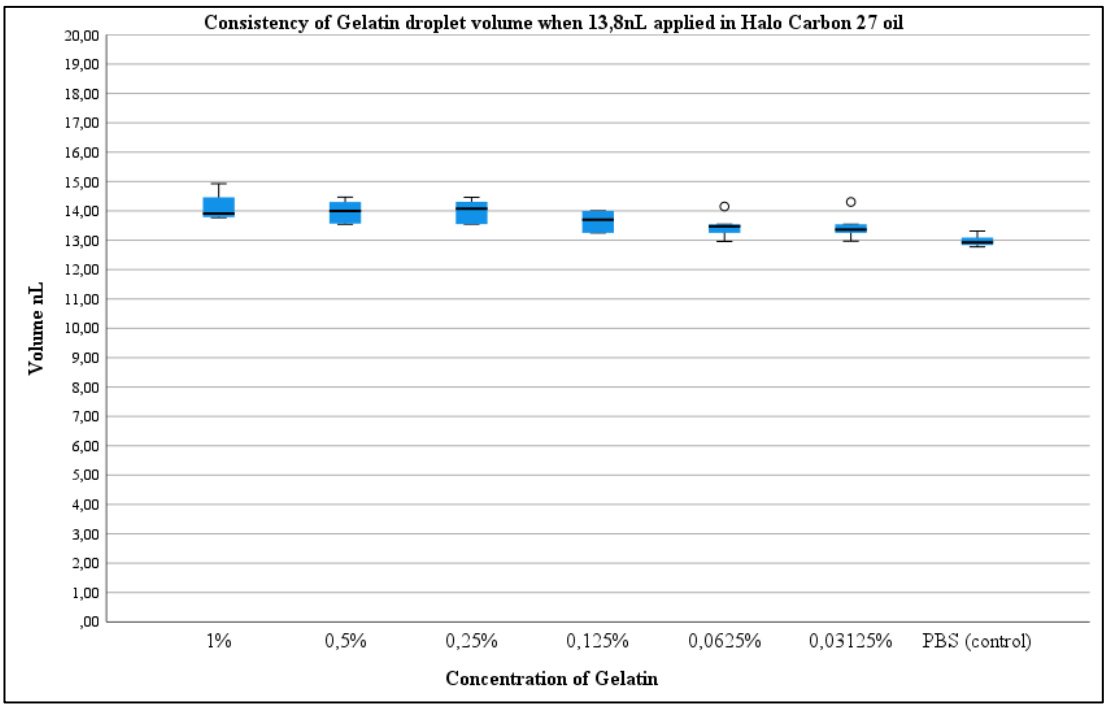

Figure 15: Variation in calculated droplet volumes with decreasing concentration of Gelatin compared to the PBS control *(M* = 12.96*, SD* = 0.19*)*: Gelatin 1% (*M* = 12.25, *SD* = 0.73), 0.5% (*M* = 14.14, *SD* =0.62), 0.25% (*M* = 13.92, *SD* = 0.61), 0.125% (*M* = 13.71, *SD* = 0.63), 0.0625% (*M* = 13.59, *SD* = 0.60), and 0.03125% (*M* = 13.38, *SD* = 0.66).

No significant differences were found between the droplet volumes between different concentrations of Gelatin and the PBS control (F (5;48) = 2.386; p = 0.05). The other matrixes (Grow-Dex®, Matrigel®, PureCol®, and Fibronectin) showed more considerable alterations in comparison to PBS, but only Matrigel® deviated persistently throughout all concentrations (Figure 16). However, due to the calibration method using viscous and lipophobic matrixes submerged in oil, the differences could partly be a consequence of technical issues during measurement.

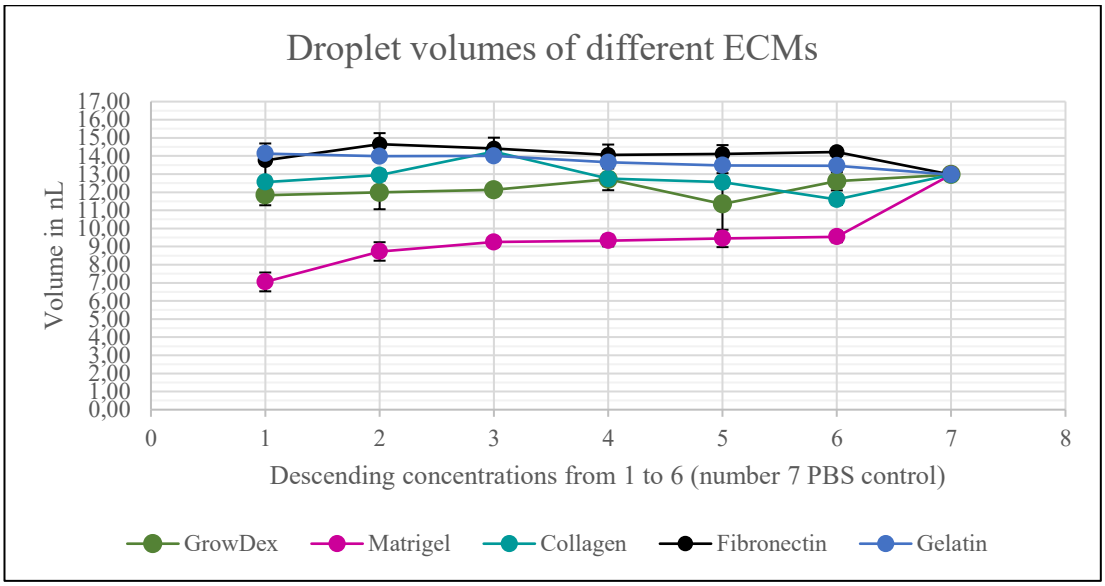

Figure 16: Plotted ECMs for comparison. The microinjected Matrigel® droplets showed to be consistently smaller compared to the other matrixes throughout all the different concentrations of matrix media (see Table 1 on page 26 for exact concentrations).

5.2 Mitochondrial DNA can be targeted for quantification of MDA-MB-231 mCherry from xenografted zebrafish embryos

The dilution series of 1:10 gave a rough range on the amount of MDA-MB-231 mCherry tumor cells needed to be present in the original sample for signal detection. The qPCR standard curves detecting mitochondrial and nuclear DNA from MDA-MD-231 mCherry dilution series, indicate that mitochondrial DNA could be a target abundant enough for sensitive measurements of human-originated MDA-MB-231 cells from single embryo xenograft samples (Figure 17A). The signal for amplified nuclear sequences required thermal cycles breaching the limits considered acceptable for reliable results (Figure 17B). With some modifications and narrowing down of the dilution series, the mitochondrial DNA on the other hand could be useful for quantitative MDA-MB-231 mCherry cancer cell measurements in this type of experiment.

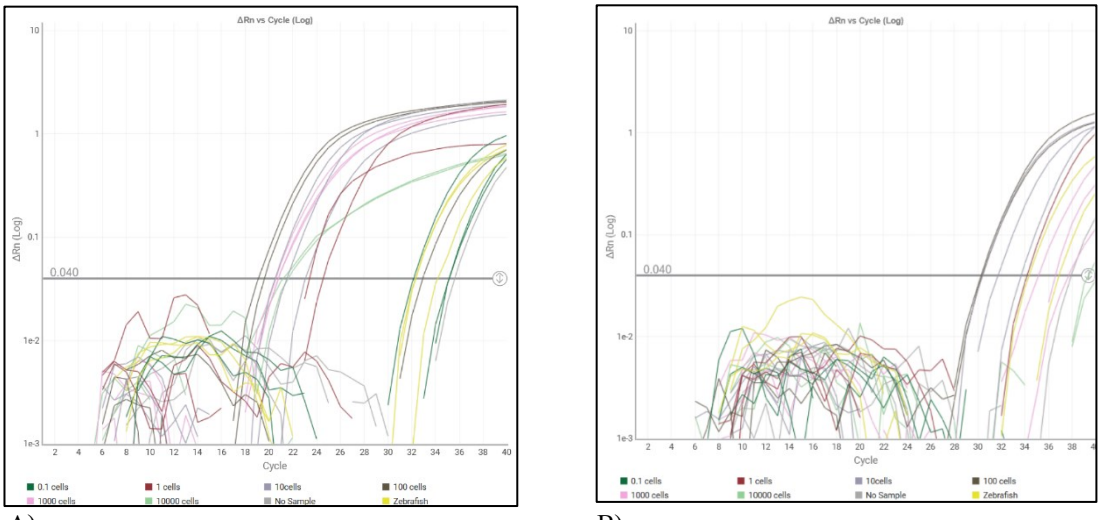

A) B)

Figure 17: The qPCR curves and cycle thresholds of 1:10 dilution series detecting A) mitochondrial DNA and B) nuclear DNA from MDA-MB-231 mCherry tumor cells indicate mitochondrial DNA being a more prominent target for quantification from single zebrafish embryo samples.

5.3 The correlation between xenograft imaging data and qPCR

The cycle threshold values for qPCR detecting mitochondrial gene sequences, done on the DNA extracts from the xenografted embryos were compared to the fluorescent intensity of each embryo (Figure 18). A moderate correlation could be found, but the results did not meet statistical significance (r (16) = 0.429, bootstrap 95% BCa CI [-0.27-0.755], p = 0.111), which led to the decision to use the well-established imaging protocols for the subsequent experiments combining the tumor cells with the ECMs.

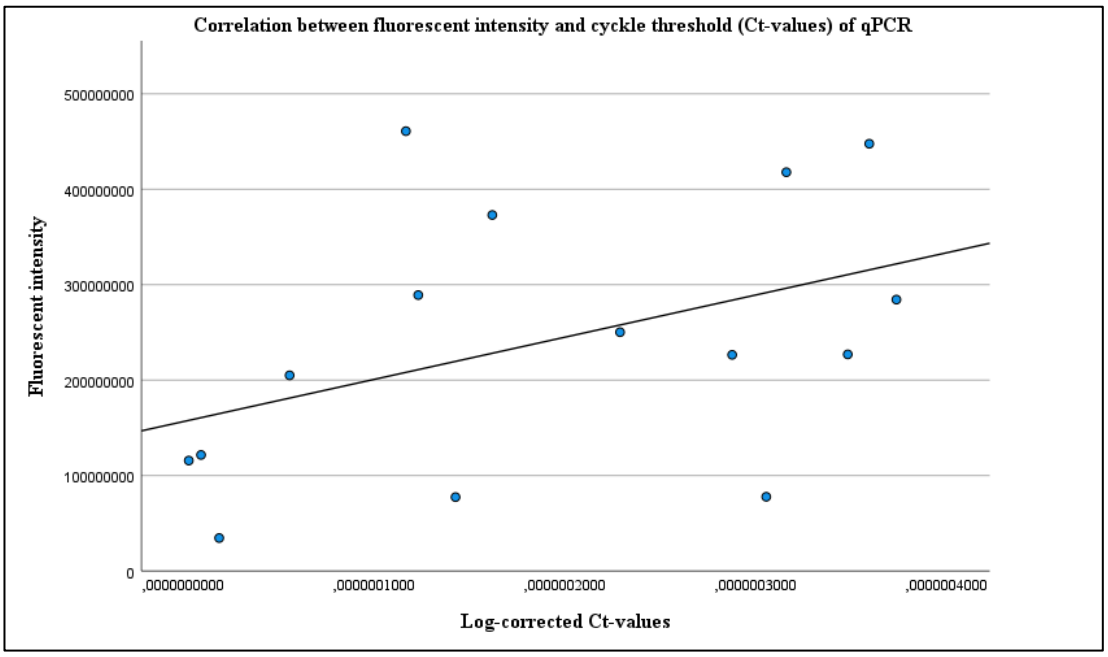

Figure 18: The correlation between the fluorescent intensity and the cycle threshold (Ct) values of qPCR, shows a moderate but statistically non-significance correlation (r (16) = 0.429; bootstrap 95% BCa CI [-0.27-0.755], p = 0.111).

5.4 ECMs as MDA-MB-231 mCherry xenograft support in zebrafish

To measure what effects ECMs have on the zebrafish xenograft, each ECM was mixed in equal concentrations with MDA-MB-231 mCherry tumor cells, and the differences in the tumor size, growth, and amounts of migrating cells were then analyzed. The results were compared with PBS as the control group.

5.4.1 Matrigel® gave larger primary tumors but did not enhance fold change

Fluorescent intensity of the 100milj/ml MDA-MB-231 mCherry tumor xenografts in zebrafish embryo 1-day post-injection resulted in larger primary tumors in the Matrigel® 9.8mgml group (n=20) (*Mdn* = 184451558.3, *IQR* = 201537167.7) compared to the PBS control group (n=20) (*Mdn* = 95283996.07, *IQR* = 167795619.1) (Figure 19A). The effect size was in the range of medium-high and statistically significant ($U = 311{,}0$, $z = 3.003$, $p = 0.002$, $r = 0.47$). The primary tumors remained larger at 4 days post-injection in the Matrigel® group (*Mdn* = 224952209.4, *IQR*= 235893151,3) compared to the PBS group (*Mdn* = 24635817.21, *IQR* = 190766786.7) but the difference in effect size diminished ($U = 289$; $z = 2.407$; $p = 0.015$; $r = 0.38$) (Figure 19B).

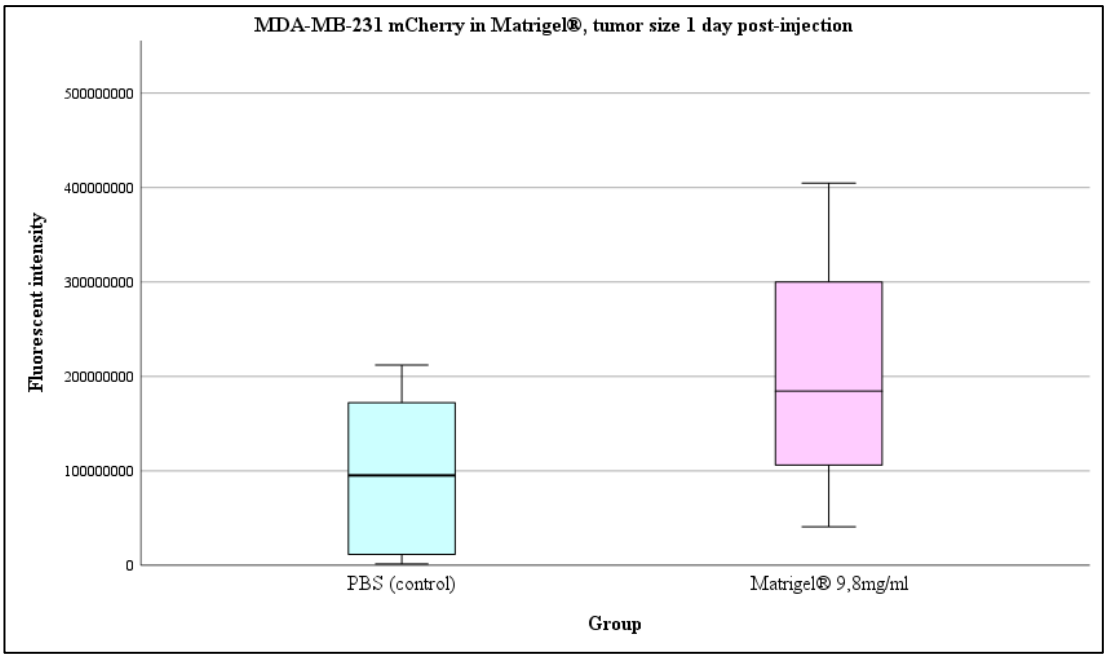

Figure 19 A): Size difference measured in fluorescent intensity of MDA-MB-231 mCherry tumors injected with Matrigel® vs. PBS (control) one-day post-injection. Xenograft solution containing Matrigel® showed tumors twice the size compared to the ones injected with only PBS (phosphate-buffered saline).

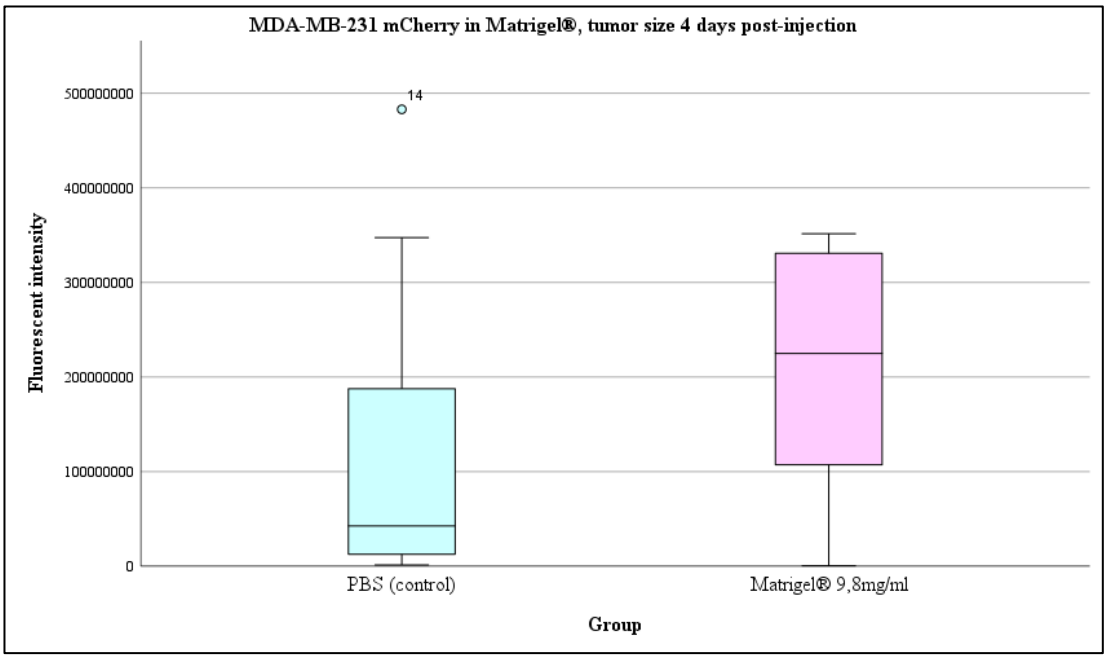

Figure 19B: The xenografted tumors measured by fluorescent intensity 4 days post-injection. The average intensity of the PBS group got larger, while the size of the Matrigel® group got smaller compared to day one.

The change in fluorescent intensity between 1dpi and 4dpi calculated from each embryo in the Matrigel® (N=20) and the PBS control group (N=20), showed no statistically significant growth rate advantage for either group (Figure 20). The fold change of fluorescence over the 4-day incubation period was larger in the PBS group (*Mdn* = 1.24, *IQR* = 1.50;) compared to the Matrigel® group (*Mdn* = 1.14, *IQR* =1.14), but the minute difference did not reach statistical significance (*U* = 196; *z* = 0.108; *r* = 0.017; *p* = 0.925) (Figure 20).

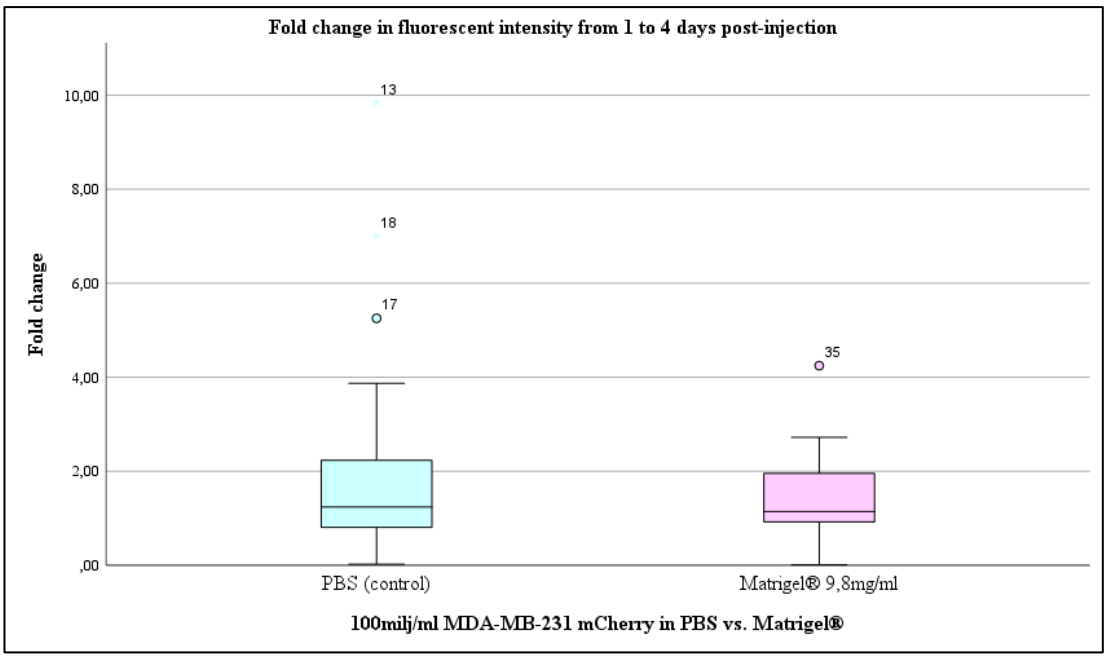

Figure 20: The tumor cells xenografted in Matrigel® solution gave larger initial tumors but no additional growth rate benefit under the days of incubation. Comparing the fold change based on fluorescent intensity between 1dpi to 4dpi, showed no statistically significant difference between the groups where MDA-MB-231 mCherry cancer cells were injected with either PBS or Matrigel® (*U* = 196; *z* = 0.108; *r* = 0.017; *p* = 0.925).

5.4.2 Comparing PureCol®, Fibronectin, and Gelatin

Measured by the fluorescence emitted by the tumor cells 1dpi, the xenografts showed a higher success rate in the groups where the MDA-MB-231 mCherry solution was fortified with PureCol® and Gelatin 1% (Figure 21). The size difference was statistically significant (H (3) = 52.96 $p < 0.001$), and the fluorescence was highest in the Gelatin 1% group (Mdn = 4808.84, IQR = 4704.53) followed by Collagen 0.232% (Mdn = 2366.18, IQR = 1988.94) and PBS (Mdn = 92.61, IQR=191.52) (Figure 21). The xenografts injected with MDA-MB-231 mCherry in Fibronectin 5µl/ml (Mdn = 112.21, IQR = 249.14) resulted in smaller grafts than the PBS control.

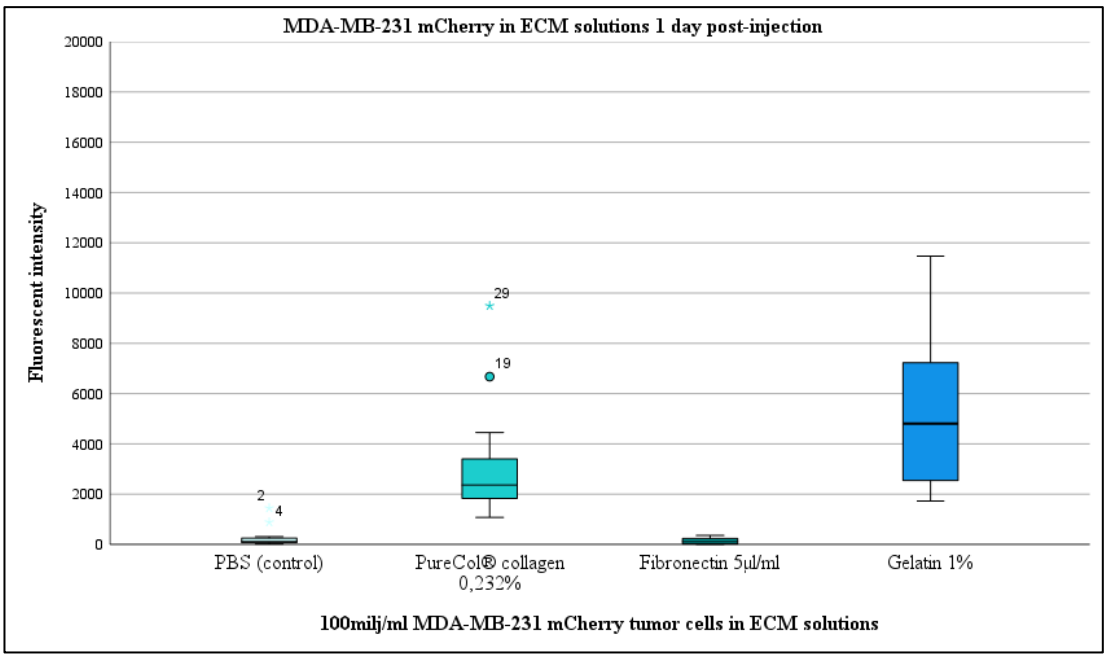

Figure 21: The MDA-MB-231 mCherry xenografts injected with PureCol® and Gelatin resulted in larger primary tumors compared to the PBS controls measured one-day post-injection. Fibronectin did not have any positive effect on the xenografts compared to PBS.

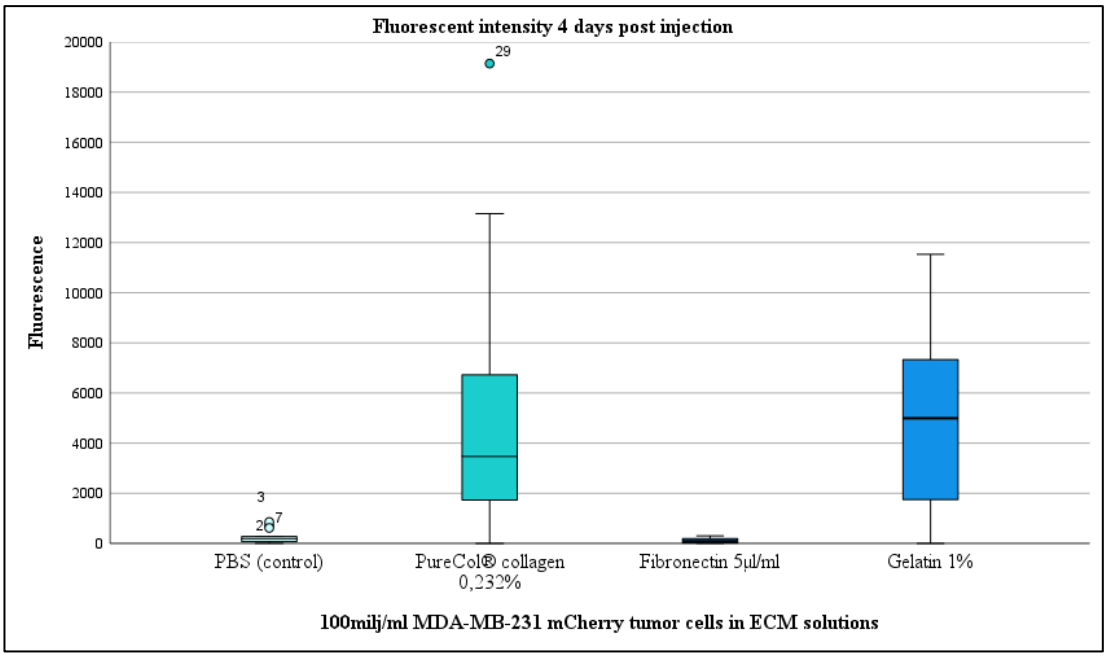

Figure 22: The MDA-MB-231 mCherry tumor cell fluorescence measured 4 days post-injection. The tumors in the PureCol® and Gelatin groups remained significantly larger, and the Fibronectin xenografts shrank from their initial size.

Interestingly, similarly to the experiments performed with Matrigel®, the larger primary tumor did not translate into larger fold-change or enhanced tumor growth when compared to PBS. The choice of xenograft media did not show to have a statistically significant effect on the fold-change (H (3) = 4.661; p = 0.198) (Figure 23). The fluorescent values by day four (*Mdn* = 238.95, *IQR* = 299.32 for PBS, *Med* = 4994.07, *IQR* = 5638.55 for Gelatin and *Med* = 3471.62, *IQR* = 5990.06 for PureCol® respectively) showed that the tumors had in average doubled in size in the PBS group (fold-change *Mdn* = 2.38, *IQR* = 3.28) while PureCol® (*Mdn* = 1.53, *IQR* = 1.97) and Gelatin (*Mdn* = 1.07, *IQR*=0.83) groups had more modest growth during the 4-day incubation period. Both Gelatin and PureCol® although significantly larger tumors 1dpi, did not grow any better than the control tumors. The size difference of the initial tumors indicates that the ECMs may have a beneficial effect on the injection procedure and the transplanting of the tumor, but for unknown reasons, the ECMs failed to provide any added growth benefit.

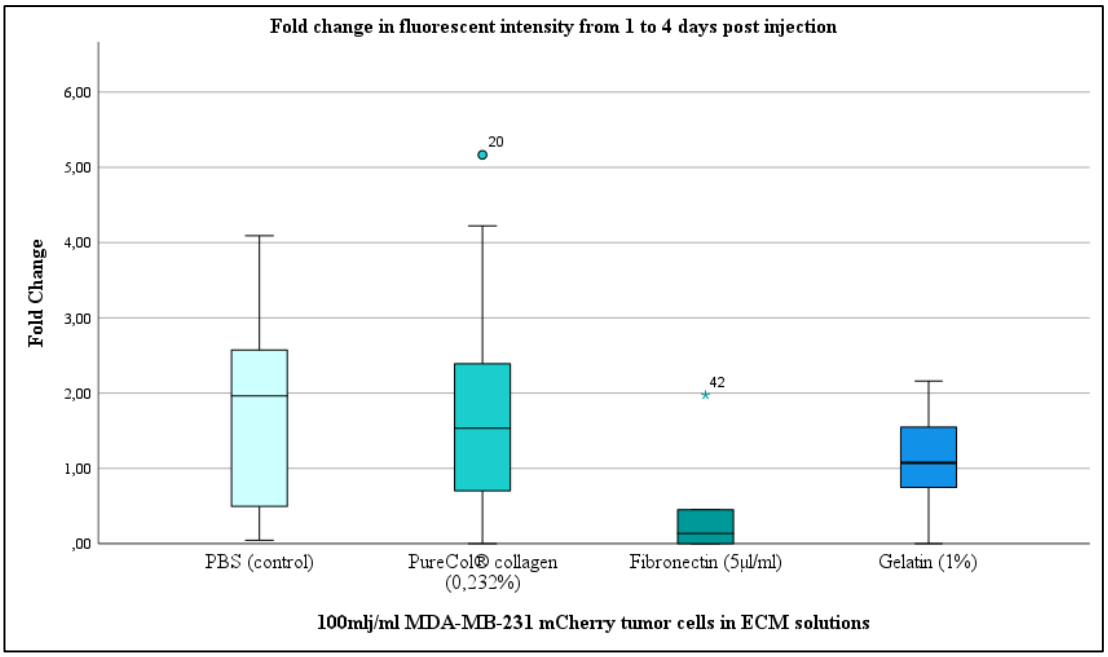

Figure 23: The fold change by day 4 was highest in the PBS group (*Mdn* = 2.38, *IQR* = 3.28), followed by PureCol® (*Mdn* = 1.53, *IQR* = 1.97), Gelatin1% (*Mdn* = 1.07, *IQR*=0.83) and Fibronectin (*Mdn* = 0.63, *IQR* = 1.58). Nevertheless, the differences were statistically non-significant (*H* (3) = 4.661, *p* = 0.198).

The two separate experiments, (PBS vs. Matrigel® and PBS vs. PureCol®, Fibronectin, and Gelatin), used different AU (arbitrary units) for fluorescent intensity, hence the difference in the orders of magnitude in the values given for the intensity in each experiment. Translating the absolute values from different modes of image conversion, cannot be performed reliably, instead pooling the relative fold changes from the two separate experiments gives a broader overview of the effects of the ECMs on tumor growth over the 4-day incubation period (Figure 24). It is worth noting that even though the fold change was not affected, a reduction in variation within the groups could be detected. A Kolmogorov-Smirnov test shows that PureCol® (*M* = 1.71; *SD* = 1,40; *D* (23) = 0.121; p > 0.200) and Gelatin (*M* = 1,06; *SD* = 0.62; *D* = (22) = 0.125; *p* > 0.200) give less variation and a more reliable normal distribution within groups, than do PBS (*M* = 1,99; *SD* = 2.02; *D* (37) = 0.193; *p* = 0.001). Comparing the samples independently against each other with a two-sample Kolmogorov-Smirnov type II test indicates that the effect of Gelatin on the reduction in variation is statistically significant (z = 1.47; *p* = 0.027).

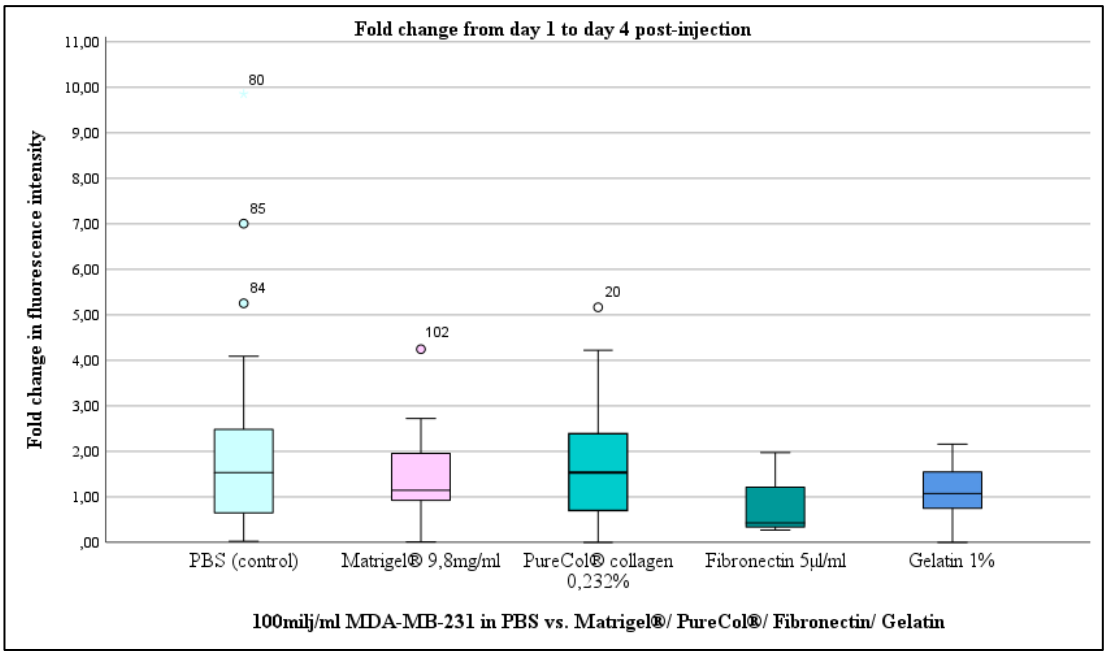

Figure 24: Pooled values of fold-change from separate experiments using different arbitrary units of fluorescent intensity. None of the ECMs enhanced the growth rate significantly compared to PBS. PureCol® and Gelatin however show to contribute to a more homogenous set of MDA-MB-231 mCherry xenografted embryos.

5.3 ECMs had no impact on tumor cells disseminating the xenograft injection site

Counting and comparing the number of tumor cells that by day 4 had escaped the original xenograft injection site, did not show any statistically significant changes when comparing PBS with the other ECM xenograft mediums (Matrigel®, PureCol®, Fibronectin, and Gelatin) (H (4) = 4.54; p=0.338) (Figure 25). The outliers with exceptionally large amounts of tumor cells in the periphery are often a result of accidentally puncturing through a circulatory blood vessel at the time of injection, rather than a sign of enhanced rate of migration of the tumor cells.

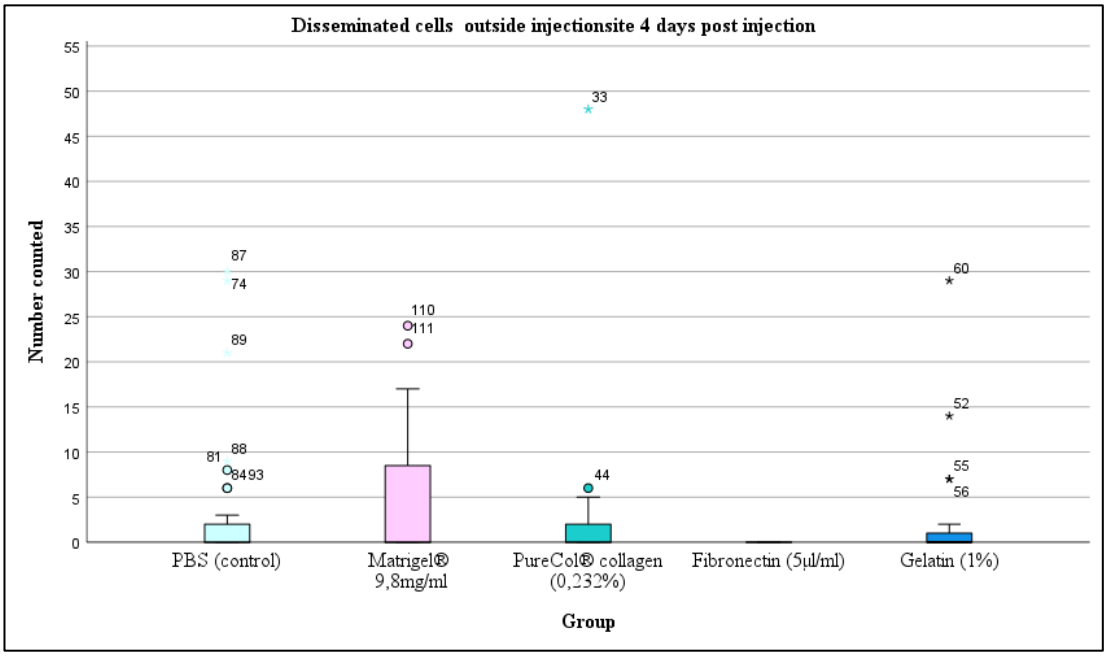

Figure 25: The amount of fluorescent MDA-MB-231 mCherry tumor cells located in tissues outside the primary injection site, did not significantly differ between the groups of tumor cells engrafted in the different xenograft media (H (4) = 4.54; p = 0.338).

6 Discussion and Conclusions

The value of zebrafish embryo xenografting in cancer research lies in its potential to provide a platform for large-scale screenings for treatment options on PDXs. Several xenograft studies have consistently demonstrated that the optimization of growth conditions for each specific cell line requires evaluation on a case-by-case basis (Fliedner et al., 2016). In the context of this study, it was observed that extracellular matrixes, namely Gelatin, could play a role in influencing the consistency and reducing the variability of MDA-MB-231 mCherry tumor xenografts in zebrafish embryos.

The method chosen for testing the droplet volumes for calibrating the microinjector for ECMs showed certain limitations. The hydraulic pressure is designed to administer a specific volume, but some of the ECM solutions sticking to the capillary needle rather than remaining under the oil surface could undeniably have affected the calculated volumes. In addition, it is worth noting that the image analysis of the droplet diameters was conducted manually, which introduces the risk of human error. Employing automated measuring software could provide added precision if this experiment were to be repeated. The issues involved with nanoliter scale microinjector calibrations have in the past been combated by using various techniques, like adding fluorescence or radioactive substances to the droplet media and plotting these results against the measured radius measurements and volume calculation (Moore et al., 2018). Another limitation of utilizing solely geometric methods is the tendency of submerged droplets to shortly take a more spherical/oval shape, thereby skewing the micrometer scale measurements. This underlines the importance of using hydrophobic dish materials to obtain more stringent calibration results (Moore et al., 2018). The preciseness of injection volumes is emphasized in situations where the dosage of for example RNA, DNA, or drugs, is crucial. Since, however, even the most concentrated ECM solutions in our experiment did not cause noticeable capillary needle clogging or blockages, the decision was made to use the most concentrated dilutions and the same settings for volume for all the different tumor+matrix xenografts. This assumption is important to keep in mind and consider as a contributing factor affecting the acquired results.

In 2019 Al-Samadi et al. evaluated the equivalence between quantification of cancer cells using imaging assays in contrast to qPCR and ddPCR (Droplet Digital PCR) measuring mRNA expression of human GADPH housekeeping genes and cytokeratin 17 (an epithelial tumor cell marker) with qPCR and ddPCR respectively, from HNSCC cell lines (Head and Neck Squamous Carcinoma Cells). The quantification methods could be deemed equally reliable, with the advantage of qPCR saving up to 4/5 of the time required for tumor cell quantification (4.6h for qPCR vs. 21.6h for fluorescent imaging and analyzing of 100 embryo samples). Using qPCR Al-Samadi et al. (2019) further evaluated the effects of eight different cancer therapies on xenografts of 4 different HNSCC cell lines and one patient-derived tumor biopsy specimen, showing varying grades of drug efficacy depending on the xenograft. This demonstrates the importance of being able to target the right tumor with the right anti-cancer agent. The limitations of quantification of tumor cells from zebrafish by fluorescence could be readily complemented by normalizing and standardizing a wider range of protocols that would be on the level with the broader toolkit of quantification methods used for murine xenograft models. In this thesis work, the quantification of MDA-MB-231 mCherry tumor cells by qPCR measuring mitochondrial DNA showed promising potential for being a target for further optimization. Working with the minimal volumes required for qPCR, normalizing the detection levels of human cells to the amount of zebrafish DNA would eliminate error rates due to residual water inevitably present in variable degrees in the single embryo samples. Al-Samadi et al. (2019) successfully utilized zebrafish GADPH housekeeping genes for this purpose. The work to finetune the protocol for MDA-MD-231 mCherry detection by qPCR was however out of the scope and time frame to be completed for this particular project, but something to be continued in the future.

Regarding the addition of ECMs as transplant support, Matrigel® used in mouse model xenografting has demonstrated its ability to enhance the “take” and growth of tumors (Benton et al., 2014). Our zebrafish experiments did not yield similar results for MDA-MB-231 mCherry growth rates, but the delicate nature of cell culturing and xenografting in general, prevents drawing overly hasty conclusions. Previous research evaluating Matrigel’s® ability to improve xenografts in conjunction with mouse models has shown to be highly selective towards certain tumor cell types (Fliedner et al., 2016). Some specific cell types have shown significant improvement in tumor take

and growth, while others have shown little to no effect on these parameters (Fliedner et al., 2016). Interestingly Matrigel® was able to deliver larger tumors in our zebrafish avatars even though, according to the droplet volume measurements, it would dispense only roughly half of the volume compared to PBS. As mentioned earlier, a more precise method of calibration would be needed to confirm the exact reason for the differences in tumor size between PBS and Matrigel®. In contrast, a separate study by Fliedner et al. 2016 investigating FaDu tumor cells (Hypopharyngeal Carcinoma) by measuring tumor size, cell density, tumor growth, and proliferation rates in the mouse model using PET scan, and tumor cell analysis by immunohistochemistry (post dissection), concluded no additional benefit of using Matrigel® for the FaDu cell line. Instead, they found that the proliferation rates were highest in the groups of smaller tumors and without Matrigel® support (Fliedner et al., 2016). Larger tumors resulted in slower growth and decelerated proliferation, confirmed by immunohistochemistry in the mouse model (Fliedner et al., 2016). Even though the zebrafish experiments in our project did not include an analysis of proliferation rates per se, the imaging results could indicate similar cellular behavior patterns for MDA-MB-231 mCherry in the zebrafish xenograft model.

The primary tumors of the PureCol® and Gelatin xenografts showed a significant size advantage compared to those injected with PBS 1 dpi. Similar to Matrigel®, this did not however translate to any improvements in the growth of the ECM-fortified xenografts over the 4-day incubation period. Even though the cell line MDA-MB-231 mCherry has a lowered propensity for contact inhibition and is highly proliferative in cell culture, it still has its growth limits when a particular cell density is reached. One conceivable explanation for the poor growth might be the overcrowding due to larger xenografts and lack of space and nutrients thereof. A speculative but nonetheless plausible cause of the larger tumor size could be the viscous properties of the ECMs. During the microinjecting of the embryos, the xenograft media builds up pressure in the yolk sac. Therefore, it is not uncommon for some of the tumor cell xenograft media to escape once the capillary needle is pulled out. The larger tumors could therefore be a logical consequence of the mechanical and technical advantages of using ECMs for xenografting, resulting in smaller amounts of media escaping the yolk sac post-injection. While microinjecting tumor cells in PBS media, the cells tend to slowly descend and accumulate towards the tip of the capillary needle, generating a risk of a

gradual reduction in the cell concentration per injection towards the end of the injection procedure. The added viscosity provided by ECMs could contribute to the cell suspension staying more homogenous in the capillary needle, leading to less variation between the xenografts. The ECM's ability to make the pool of xenografted embryos more homogenous could be considered an important benefit in itself since this would reduce the number of embryos needed to be subjected to xenografting to obtain the number of animals needed for any given experiment. It is worth noting that Gelatin, which in our experiments showed the largest benefit for a reduction in variation, is one of the most affordable ECMs. The potential of Gelatin as an addition to xenograft mediums would therefore be worthwhile to investigate further as a cost-effective aid to spare both amounts of tumor cells needed, and animals to be sacrificed in the attempt to expand zebrafish xenograft practices to PDX screenings.

To conclude, growing attention for translational biomedical research and advances in targeted therapies hold important promise in the fight against cancer. While the murine model still possesses the status as the most well-established mammalian model organism, the insights into xenograft behavior in a variety of different model organisms like the zebrafish, not only address ethical and economic considerations but could provide us with a considerably faster alternative compared to both mPDXs (murine Patient Derived Xenografts) and various *in vitro* methods. The theories about the origin and progression of cancer over the past century, from germ theory to terrain theory to the current genetic mutations approach, have in some respect reached a full circle with the growing emphasis on the microenvironment as an important contributor to tumor behavior. The pleomorphic nature of a cancer cell, shifting its survival strategies along the way and manipulating its surroundings accordingly, makes picking apart the exact marching order of events during clinical tumor development a hard nut to crack. Whatever the case may be, refining and innovating new techniques for zebrafish xenografts could advance precision oncology and facilitate quicker, easier, and more robust methods for clinical screenings of combination therapies, which today are seen as the most promising approach for effective tumor suppression. The synergistic effects of different drug combinations could be investigated directly, aiding in cost-effectiveness and rapid decision-making of whichever treatment option is best suited for each patient. In contrast to the murine models, the zebrafish xenograft model

holds promise for being utilizable for this kind of hands-on patient-oriented clinical use in the near future.

7 Acknowledgments

First, I would like to express my gratitude to my supervisor, Ph.D. Ilkka Paatero, for all the guidance and invaluable teachings of essential scientific principles throughout the course of this project. His mentorship and prep talks have been an instrumental source of motivation, encouragement, and good mood, empowering me to remain focused and approach challenges with a growth-oriented mindset. I am sincerely grateful for the opportunity to conduct my master's thesis work at the Zebrafish Core Facility at Turku Bioscience Center, the hub for joint research efforts between Åbo Akademi and the University of Turku.

I also want to thank my fellow office staff at Turku Bioscience Center, Anna-Mari Haapanen-Saaristo and Miika Niemeläinen, for their much-appreciated technical support in navigating various computational hurdles encountered during this work.

Furthermore, I would like to thank Petra Laasola, Jenni Siivonen, and Jenna Villman for their guidance and assistance during the practical laboratory work associated with my thesis.

Lastly, I would like to express my appreciation to my beloved partner and my mother. Their commitment and effort to de-burden me from household chores and walking and keeping our dog company, has greatly alleviated my feelings of guilt during the busy schedule and long days at the university campus.

8 References

Afewerki, S., Sheikhi, A., Kannan, S., Ahadian, S., & Khademhosseini, A. (2019). Gelatin-polysaccharide composite scaffolds for 3D cell culture and tissue engineering: Towards natural therapeutics. *Bioengineering & Translational Medicine*, *4*(1), 96–115. https://doi.org/10.1002/btm2.10124

Alberts, B., Heald, R., Johnson, A., Morgan, D., Raff, M., Roberts, K., & Walter, P. (2022). *Molecular Biology of the Cell* (7th ed.). W.W. Norton&Company.

Aleström, P., D'Angelo, L., Midtlyng, P. J., Schorderet, D. F., Schulte-Merker, S., Sohm, F., & Warner, S. (2020). Zebrafish: Housing and husbandry recommendations. *Laboratory Animals*, *54*(3), 213–224. https://doi.org/10.1177/0023677219869037

Al-Samadi, A., Tuomainen, K., Kivimäki, A., Salem, A., Al-Kubati, S., Hyytiäinen, A., Parikka, M., Mesimäki, K., Wilkman, T., Mäkitie, A., Grenman, R., & Salo, T. (2019). PCR-based zebrafish model for personalised medicine in head and neck cancer. *Journal of Translational Medicine*, *17*(1), 235. https://doi.org/10.1186/s12967-019-1985-1

Astell, K. R., & Sieger, D. (2020). Zebrafish In Vivo Models of Cancer and Metastasis. *Cold Spring Harbor Perspectives in Medicine*, *10*(8), a037077. https://doi.org/10.1101/cshperspect.a037077

Benton, G., Arnaoutova, I., George, J., Kleinman, H. K., & Koblinski, J. (2014). Matrigel: From discovery and ECM mimicry to assays and models for cancer research. *Engineering of Tumor Microenvironments*, *79–80*, 3–18. https://doi.org/10.1016/j.addr.2014.06.005

Benton, G., Kleinman, H. K., George, J., & Arnaoutova, I. (2011). Multiple uses of basement membrane-like matrix (BME/Matrigel) in vitro and in vivo with cancer cells. *International Journal of Cancer*, *128*(8), 1751–1757. https://doi.org/10.1002/ijc.25781

Bradford, Y. M., Toro, S., Ramachandran, S., Ruzicka, L., Howe, D. G., Eagle, A., Kalita, P., Martin, R., Taylor Moxon, S. A., Schaper, K., & Westerfield, M. (2017). Zebrafish Models of Human Disease: Gaining Insight into Human Disease at ZFIN. *ILAR Journal*, *58*(1), 4–16. https://doi.org/10.1093/ilar/ilw040

Chen, L., Groenewoud, A., Tulotta, C., Zoni, E., Kruithof-de Julio, M., van der Horst, G., van der Pluijm, G., & Ewa Snaar-Jagalska, B. (2017). A zebrafish xenograft model for studying human cancer stem cells in distant metastasis and therapy response. In *Methods in Cell Biology* (Vol. 138, pp. 471–496). Elsevier. https://doi.org/10.1016/bs.mcb.2016.10.009

Chen, X., Li, Y., Yao, T., & Jia, R. (2021). Benefits of Zebrafish Xenograft Models in Cancer Research. *Frontiers in Cell and Developmental Biology*, *9*, 616551. https://doi.org/10.3389/fcell.2021.616551

Clemence, M. (2018). *Public attitudes to animal research in 2018*. IPSOS. https://www.ipsos.com/en-uk/public-attitudes-animal-research-2018

Costa, B., Estrada, M. F., Mendes, R. V., & Fior, R. (2020). Zebrafish Avatars towards Personalized Medicine—A Comparative Review between Avatar Models. *Cells*, *9*(2), 293. https://doi.org/10.3390/cells9020293

Dillekås, H., Rogers, M. S., & Straume, O. (2019). Are 90% of deaths from cancer caused by metastases? *Cancer Medicine*, *8*(12), 5574–5576. https://doi.org/10.1002/cam4.2474

Fior, R., Póvoa, V., Mendes, R. V., Carvalho, T., Gomes, A., Figueiredo, N., & Ferreira, M. G. (2017). Single-cell functional and chemosensitive profiling of combinatorial colorectal therapy in zebrafish xenografts. *Proceedings of the National Academy of Sciences*, *114*(39). https://doi.org/10.1073/pnas.1618389114

Fliedner, F. P., Hansen, A. E., Jørgensen, J. T., & Kjær, A. (2016). The use of matrigel has no influence on tumor development or PET imaging in FaDu human head and neck cancer xenografts. *BMC Medical Imaging*, *16*(1), 5. https://doi.org/10.1186/s12880-016-0105-4

Gordon, M. K., & Hahn, R. A. (2010). Collagens. *Cell and Tissue Research*, *339*(1), 247–257. https://doi.org/10.1007/s00441-009-0844-4

Hanai, K., Kojima, T., Ota, M., Onodera, J., & Sawada, N. (2012). Effects of Atelocollagen Formulation Containing Oligonucleotide on Endothelial Permeability. *Journal of Drug Delivery*, *2012*, 1–9. https://doi.org/10.1155/2012/245835

Hason & Bartůněk. (2019). Zebrafish Models of Cancer—New Insights on Modeling Human Cancer in a Non-Mammalian Vertebrate. *Genes*, *10*(11), 935. https://doi.org/10.3390/genes10110935

Howe, K., Clark, M. D., Torroja, C. F., Torrance, J., Berthelot, C., Muffato, M., Collins, J. E., Humphray, S., McLaren, K., Matthews, L., McLaren, S., Sealy, I., Caccamo, M., Churcher, C., Scott, C., Barrett, J. C., Koch, R., Rauch, G.-J., White, S., … Stemple, D. L. (2013). The zebrafish reference genome sequence and its relationship to the human genome. *Nature*, *496*(7446), 498–503. https://doi.org/10.1038/nature12111

Huang, Z., Yu, P., & Tang, J. (2020). Characterization of Triple-Negative Breast Cancer MDA-MB-231 Cell Spheroid Model. *OncoTargets and Therapy*, *Volume 13*, 5395–5405. https://doi.org/10.2147/OTT.S249756

Insua-Rodríguez, J., & Oskarsson, T. (2016). The extracellular matrix in breast cancer. *Advanced Drug Delivery Reviews*, *97*, 41–55. https://doi.org/10.1016/j.addr.2015.12.017

Karamanos, N. K., Theocharis, A. D., Piperigkou, Z., Manou, D., Passi, A., Skandalis, S. S., Vynios, D. H., Orian-Rousseau, V., Ricard-Blum, S., Schmelzer, C. E. H., Duca, L., Durbeej, M., Afratis, N. A., Troeberg, L., Franchi, M., Masola, V., & Onisto, M. (2021). A guide to the composition and functions of the extracellular matrix. *The FEBS Journal*, *288*(24), 6850–6912. https://doi.org/10.1111/febs.15776

Lee, S. L. C., Rouhi, P., Jensen, L. D., Zhang, D., Ji, H., Hauptmann, G., Ingham, P., & Cao, Y. (2009). Hypoxia-induced pathological angiogenesis mediates tumor cell dissemination, invasion, and metastasis in a zebrafish tumor model. *Proceedings of the National Academy of Sciences*, *106*(46), 19485–19490. https://doi.org/10.1073/pnas.0909228106

Lepucki, A., Orlińska, K., Mielczarek-Palacz, A., Kabut, J., Olczyk, P., & Komosińska-Vassev, K. (2022). The Role of Extracellular Matrix Proteins in Breast Cancer. *Journal of Clinical Medicine*, *11*(5), 1250. https://doi.org/10.3390/jcm11051250

Li, Z., Ptak, D., Zhang, L., Walls, E. K., Zhong, W., & Leung, Y. F. (2012). Phenylthiourea Specifically Reduces Zebrafish Eye Size. *PLoS ONE*, *7*(6), e40132. https://doi.org/10.1371/journal.pone.0040132

Maity, G., Choudhury, P. R., Sen, T., Ganguly, K. K., Sil, H., & Chatterjee, A. (2011). Culture of human breast cancer cell line (MDA-MB-231) on fibronectin-coated surface induces pro-matrix metalloproteinase-9 expression and activity. *Tumor Biology*, *32*(1), 129–138. https://doi.org/10.1007/s13277-010-0106-9

Miladinov, V., Gennadios, A., & Hanna, M. (2002). *Gelatin Manufacturing Process and Product*.

Minakuchi, Y. (2004). Atelocollagen-mediated synthetic small interfering RNA delivery for effective gene silencing in vitro and in vivo. *Nucleic Acids Research*, *32*(13), e109–e109. https://doi.org/10.1093/nar/gnh093

Moore, C. L., Taylor, E. M., Ball, K. K., Bernock, L. J., Griffin, R. J., Jung, S., Shoeib, A., & Borrelli, M. J. (2018). Quantitative microinjection using fluorescence calibration of streaming microdroplets on a superhydrophobic surface. *Experimental Cell Research*, *370*(2), 426–433. https://doi.org/10.1016/j.yexcr.2018.07.006

Mouw, J. K., Ou, G., & Weaver, V. M. (2014). Extracellular matrix assembly: A multiscale deconstruction. *Nature Reviews Molecular Cell Biology*, *15*(12), 771–785. https://doi.org/10.1038/nrm3902

Nakayama, J., Makinoshima, H., & Gong, Z. (2022). Gastrulation Screening to Identify Anti-metastasis Drugs in Zebrafish Embryos. *BIO-PROTOCOL*, *12*(19). https://doi.org/10.21769/BioProtoc.4525

Nimesh, S. (2013). Atelocollagen. In *Gene Therapy* (pp. 225–235). Elsevier. https://doi.org/10.1533/9781908818645.225

Paolillo & Schinelli. (2019). Extracellular Matrix Alterations in Metastatic Processes. *International Journal of Molecular Sciences*, *20*(19), 4947. https://doi.org/10.3390/ijms20194947

Quail, D. F., & Joyce, J. A. (2013). Microenvironmental regulation of tumor progression and metastasis. *Nature Medicine*, *19*(11), 1423–1437. https://doi.org/10.1038/nm.3394

Roth, S. M., Berens, E. B., Sharif, G. M., Glasgow, E., & Wellstein, A. (2021). Cancer Cell Invasion and Metastasis in Zebrafish Models (Danio rerio). In U. S. Stein (Ed.), *Metastasis* (Vol. 2294, pp. 3–16). Springer US. https://doi.org/10.1007/978-1-0716-1350-4_1

Sadava, D., Hillis, D. M., Heller, H. C., & Berenbaum, M. R. (2012). *Life: The science of biology* (10th edition, 1st printing). Sinauer.

Schaefer, L., & Schaefer, R. M. (2010). Proteoglycans: From structural compounds to signaling molecules. *Cell and Tissue Research*, *339*(1), 237–246. https://doi.org/10.1007/s00441-009-0821-y

Su, K., & Wang, C. (2015). Recent advances in the use of gelatin in biomedical research. *Biotechnology Letters*, *37*(11), 2139–2145. https://doi.org/10.1007/s10529-015-1907-0

Travnickova, J., Nhim, S., Abdellaoui, N., Djouad, F., Nguyen-Chi, M., Parmeggiani, A., & Kissa, K. (2021). Macrophage morphological plasticity and migration is Rac signalling and MMP9 dependant. *Scientific Reports*, *11*(1), 10123. https://doi.org/10.1038/s41598-021-88961-7

Vitale, C., Marzagalli, M., Scaglione, S., Dondero, A., Bottino, C., & Castriconi, R. (2022). Tumor Microenvironment and Hydrogel-Based 3D Cancer Models for In Vitro Testing Immunotherapies. *Cancers*, *14*(4), 1013. https://doi.org/10.3390/cancers14041013

Walker, C., Mojares, E., & del Río Hernández, A. (2018). Role of Extracellular Matrix in Development and Cancer Progression. *International Journal of Molecular Sciences*, *19*(10), 3028. https://doi.org/10.3390/ijms19103028

Weinberg, R. A. (2014). *The Biology of Cancer* (2nd ed.). Garland Science.

Welsh, J. (2013). Animal Models for Studying Prevention and Treatment of Breast Cancer. In *Animal Models for the Study of Human Disease* (pp. 997–1018).

White, R. M., Sessa, A., Burke, C., Bowman, T., LeBlanc, J., Ceol, C., Bourque, C., Dovey, M., Goessling, W., Burns, C. E., & Zon, L. I. (2008). Transparent Adult Zebrafish as a Tool for In Vivo Transplantation Analysis. *Cell Stem Cell*, *2*(2), 183–189. https://doi.org/10.1016/j.stem.2007.11.002

Yan, C., Brunson, D. C., Tang, Q., Do, D., Iftimia, N. A., Moore, J. C., Hayes, M. N., Welker, A. M., Garcia, E. G., Dubash, T. D., Hong, X., Drapkin, B. J., Myers, D. T.,

Phat, S., Volorio, A., Marvin, D. L., Ligorio, M., Dershowitz, L., McCarthy, K. M., … Langenau, D. M. (2019). Visualizing Engrafted Human Cancer and Therapy Responses in Immunodeficient Zebrafish. *Cell*, *177*(7), 1903-1914.e14. https://doi.org/10.1016/j.cell.2019.04.004

Yoshida, G. J. (2020). Applications of patient-derived tumor xenograft models and tumor organoids. *Journal of Hematology & Oncology*, *13*(1), 4. https://doi.org/10.1186/s13045-019-0829-z

9 Appendix I

Calibration

Needle puller: GWB Narishige Japan PB-7 Capillaries: 3,5” Drummond # 3-000-203-g/X glass capillaries from Drummond Scientific USA

Halocarbon Oil 27 for calibration, Sigma-Aldrich, Batch MKBG 0880

Mineral oil for microinjector (light) d: 0,84/ml (at 25 °C) Cas. 8042-47-5, Lot MKBT2494V

Matrixes

Grow-Dex® 1,5% UPM Ref: 100 103 002, Lot. 121791922, Exp. 08-2023

Matrigel® Matrix GFR (growth factor reduced) 19,60mg/ml, Ref. 354263, Lot 0013005

PureCol®, Inamed BioMaterials, Lot. 5409187631, Exp. 01-2009

Fibronectin 1mgml, Bovine Plasma 341631-5mg Sigma-Aldrich

Gelatin® from porcine skin, Gel Strength 300 Type A Gelatin, Sigma-Aldrich, Lot SLCC7838

Phenol Red sol. 0,5%, Sigma-Aldrich, Lot. RNBK6526

MDA-MB-231 cell culturing

Tumor Cell line MDA-MB-231 mCherry (28.5.2020 P3 dens. ½ 10cm),

DMEM, Dulbecco’s Modified Eagle Medium, High glucose sterile filtered, Batch: VWRM501MF, Exp. Nov-29-2024

Cell culture media	200ml
DMEM- media, High Glucose	176ml
Fetal Bovine Serum	20ml
Penicillin-Streptomycin	2ml
L-Glutamine	2ml

Innovatis Cedex 3271 XS cell counter

Zebrafish culturing

Embryo Media (E3+ PTU)	1000ml
E3 60X stock	16.6ml
Penicillin-Streptomycin (100x)	10ml
Phenylthiourea 20mM stock	10ml
Methylene Blue (50 000xStock)	25µl
H_2O	Ad 1000ml

E3 stock (60X)	500ml
NaCl	8.6g
KCl	0.8g
$CaCl_2*2H_2O$	1.45g
$MgSo_4*7H_2O$	2.45g
H_2O	Ad 500g

Pronase E ® SELVA# 33635.02 Lot. 150369 09.11-2016

MS-222 zebrafish sedative: 1% Tricaine Methanesulfonate+ 0,002% Tween-20

1,5% Agarose for zebrafish mounting dishes Agarose Molecular Grade, REF. 41025, Lot: ES520-B093230

PowerUP™ SYBR™ Green Master Mix, Thermo Fisher Scientific, Applied Biosystems, Ref. A25741, Lot. 00843197, Exp. 31.10.2020

Oligonucleotide primers for qPCR by Integrated DNA Technologies: Hs_mtDNA-F1 5'-ACA CCC TCC TAG CCT TAC TAC-3' Hs_mtDNA-R1 5'-GAT ATA GGG TCG AAG CCG C-3' Hs_nucleusDNA F1 5'- AGGGTA TCT GGG CTC TGG-3' Hs_nucleusDNA R1 5'-GGC TGA AAA GCT CCC GAT TAT-3'

10 Summary in Swedish- Svensk Sammanfattning

—*Danio rerio*—
Extracellulära matriser och cancercellväxt i xenograftmodellen för zebrafisk

1 Bakgrund och introduktion

Zebrafisken —*Danio rerio*— är en liten sötvattensfisk, som varit föremål för olika vetenskapliga tillämpningar sedan de första försöken utfördes av George Streisinger på 1960-talet (Astell &; Sieger, 2020; Bradford et al., 2017). Forskningsmetoderna på den tiden var enkla, och bestod främst av observationsstudier av tidig embryogenes, och hur tidig utveckling kan störas av embryotoxiska medel (Bradford et al., 2017). Metoderna för toxicitetsscreening används fortfarande i vid utsträckning till denna dag, men zebrafiskforskning har utvidgats till att utnyttja också många av de moderna tekniker som baserar sig på fynden inom genetik och molekylärbiologi (Bradford et al., 2017).

Fastän zebrafisken inte är ett däggdjur, är den i många avseende i sin anatomi och genetik mycket användbar för studier relaterade till människans biologi och sjukdomstillstånd. Zebrafiskens genom på cirka 26 000 proteinkodande gener har 72 % ortologi med människans genom, och upp till 82 % då det gäller sjukdomsorskakande gener (Howe et al., 2013). De nya uppfinningarna inom molekylärbiologi såsom CRISPR-Cas9-tekniken, morfoliner och interfererande RNA (eng. interfering RNA), har dessutom möjliggjort genetiska manipulationer såsom knock-outs, knock-ins och knock-downs, som kan användas för att spåra hur nedtystning/ addering av olika gener och proteinuttryck påverkar zebrafisken. Denna kunskap har använts för att avsiktligt skapa specifika mutationer, varvid det idag finns en uppsättning av olika zebrafiskstammar som imiterar motsvarande sjukdomstillstånd

hos människan (Astell &; Sieger, 2020; Nakayama et al., 2022). Muterade pigmentgener har möjliggjort en stam av albinozebrafiskar (Casper), och genteknologiska modifikationer som uttrycker vävnadsspecifika fluorescerande proteiner kan användas för att följa med till exempel vaskulär eller neuronal utveckling i realtid i ett levande embryo (White et al., 2008). Detta har bidragit till att Casper-stammens zebrafisk har ökat i popularitet som ett *in vivo*-forskningsobjekt hand i hand med den snabbt framskridande utvecklingen av allt mer avancerad teknik för fluorescensmikroskopering (White et al., 2008).

Ett problem inom dagens cancerforskning utgörs av det faktum att många effekter som observeras i *in vitro*-cellodlingar inte korrelerar med effekterna då försöken fortgår till kliniska studier i *in vivo*-system (Bradford et al., 2017). Både terapeutiska och toxiska effekter kan utrycka sig väldigt annorlunda i en levande organism jämfört med cellkulturer. Försök gjorda på däggdjur som mus och råtta är förutom kostsamma, också etiskt problematiska och därmed strikt reglerade (Nakayama et al., 2022). Zebrafiskxenograftmodellen för cancer strävar till att kunna fungera som ett kostnadseffektivt mellansteg för grov sållning av toxiska och ineffektiva alternativ, innan fortsatta djurförsök på högre orderns organismer (Nakayama et al., 2022). Den heterogena sammansättningen på genmutationer hos varje enskild cancerpatient ställer stora krav på en mångsidig uppsättning av behandlingsstrategier. Hoppet är att zebrafiskxenograftmodellen i framtiden kunde användas som en *in vivo*-modell för storskalig PDX-screening (patient-härledd xenograft, eng. Patient Derived Xenograft), det vill säga som ett verktyg inom personlig medicin på patientspecifika biopsiprov.

ECM, den extracellulära matrisen och tumörnischen har visat sig ha en nyckelroll i hur cancer framskrider och metastaserar (Paolillo & Schinelli, 2019). ECM-komponenter används i dagens läge allmänt i *in vitro*-cellkulturer och organoidkulturer, men i viss utsträckning också i murinmodeller, då ECM: s förmåga att påverka cellers överlevnad och proliferationsförmåga undersöks. I detta slutarbete kartläggs hur ECM kan användas i samband med microinjicering av zebrafiskembryoxenografter, samt vilken effekt dessa ECM har på MDA-MB-321 mCherry tumörtransplantat. Dessutom är syftet att undersöka alternativa metoder för detektion av MDA-MB-231 mCherry tumörer i zebrafiskcancermodellen, som idag vanligen utförs med hjälp av arbetsdryg fluorescensmikroskopering och bildanalys.

2 Material och metoder

För projektet valdes allmänt använda kommersiella ECM; Grow-Dex®, Matrigel®, PureCol® kollagen, Fibronectin och Gelatin. Dessa testades i olika koncentrationer tillsammans med mikroinjektionsutrustning för att bilda en uppfattning om huruvida de viskösa matriserna är användbara tillsammans med kapillärnålar och de minimala volymer som zebrafisktumörtransplantering kräver. En aggressiv metastaserande cellinje av MDA-MB-231 mCherry bröstcancer (duktalt adenocarcinom) användes för att undersöka ifall tillägg av olika ECM i xenograftmediet påverkar tumörväxten i jämförelse till fosfatbuffrad salinlösning, PBS (eng. Phosphate Buffered Saline). Som huvudmetod för detektering av humana cancerceller i zebrafiskembryot användes väletablerade metoder baserade på fluorescensmikroskopering och bildanalys med Fijis ImageJ programvara.

Som en alternativ detektionsmetod till mikroskopering testades kvantitativ polymeras kedjereaktion, qPCR (eng. quantitative Polymerase Chain Reaction), med två olika primärsekvenser, en för humanspecifikt mitokondriellt DNA samt en för humanspecifikt nukleärt DNA. Dessa utvaldes på grund av att de kunde tänka sig finnas i MDA-MB-231 mCherry tumörcellerna i mängder stora nog för att med tillräcklig specificitet och känslighet kunna detekteras i ett zebrafiskembryosampel med hjälp av qPCR. Resultaten från bildanalys på fluorescensstyrka samt qPCR på DNAt extraherat från det hela zebrafiskembryosamplet användes sedan för korrelationsanalys.

Alla matriser förutom Grow-Dex® valdes för att testas som medium i zebrafiskxenografter då zebrafiskembryona injicerades med fluorescerande cancerceller 2dpf (dagar efter befruktning, eng. Days Post Fertilization). Embryona fotograferades 1dpi (dagar efter injektion, eng. Days Post Injection) och 4dpi varefter tumörstorleken mätt på basis av fluorescensintensitet jämfördes mellan de olika matrisgrupperna för att undersöka ifall matrisstödstrukturer i injiceringsmediet påverkar tumörernas tillväxthastighet eller mängden celler som kan hittas utanför själva injektionsstället.

3 Resultat och diskussion

De undersökta matriserna (med undantag av Grow-Dex®) visade sig fungera ihop med utrustningen för microinjicering och oron över blockering av kapillärnålen visade sig vara obefogad. Kalibreringsförsöket av injektionsvolymer visar en del spridning, men på grund av att metoden med viskösa matriser tillsammans med hydrofob kalibreringsolja visade sig suboptimal för detta ändamål, är den grundläggande orsaken till spridningen omöjlig att fastställa.

Mängden av det humanspecifika nukleära DNAt i MDA-MB-231 mCherry visad sig i den kvantitativa polymeraskedjereaktionen underskrida det som vore optimalt för ett lågt och därmed pålitligt cykeltröskelvärde med de tumörcellskoncentrationer som kan förväntas i ett embryosampel. qPCR-standardkurvorna för MDA-MB-231 mCherry indikerar däremot att mängden mitokondriellt DNA i tumörcellerna är i storleksordning med de volymer och koncentrationer som kunde erhållas från ett zebrafiskembryosampel. Detta var ett grovt experiment för att hitta en lämplig gensekvens som lämpar sig för genamplifiering av MDA-MB-231 mCherry humanceller ur ett singel embryosampel. Fortsatta försök kunde arbeta med att optimera standardkurvan genom att minska på spädningsfaktorn och finslipa koncentrationerna. Dessutom kunde testet normaliseras genom att mäta också signalen från själva zebrafiskembryot, varvid de två värden skulle förhålla sig i relation till varandra, och resterande vatten i samplen inte skulle påverka resultatet. På så vis kunde man möjligtvis uppnå en precis räckvidd för kvantitativ mätning av mängden MDA-MB-231 tumörceller i ett zebrafiskembryosampel.

Korrelationsanalysen mellan fluorescensintensitet och cykeltröskel värdet (Ct-värdet) på mitokondriellt DNA i qPCR, visade ett moderat men ett icke statistiskt signifikant samband (r (16) =0,429; bootstrap 95% BCa CI [-0,27-0,755]; p = 0,111). Testet kunde upprepas med större sampelstorlek och företrädesvis ett bildanalyssofta optimerat för just detta ändamål. Den ovannämnda justeringen av standardkurvorna för MDA-MB-231 mCherry tumörcelldetektering kunde också bidra till att mer robusta resultat kunde uppnås, och metoden således bli pålitlig och användbar.

Cancerxenografter där PureCol® och Gelatin användes som injiceringsmedium i stället för PBS (kontroll) visade signifikant större tumörer dag 1 och dag 4 efter injicering. Den huvudsakliga orsaken till detta antas vara den fördelaktiga konsistensen på injektionsmediet. Trycket som bildas i zebrafiskembryots gulesäck (eng. yolk sac) efter injektion leder ofta till att en del av det injicerade tumörcellsmediet läcker ut genom sticksåret, varvid ett mer visköst media ser ut att effektivt hämma detta läckage. Jämförelsen mellan det som är av större relevans, *förändringen* (eng. fold change) som sker i tumörens storlek under 4 dagars inkubation, visade dock ingen statistiskt signifikant fördel för någon av ECM-grupperna. Även om primärtumörerna dag 1 var betydligt mycket mindre i PBS-gruppen, hade de i medeltal högsta relativa tillväxthastighet under inkubationstiden. Det gick heller inte att påvisa statistiskt signifikanta skillnader i mängden tumörceller som extravaserar från primärtumören och migrerar till distala vävnader inom grupperna som injicerats med tumörceller i olika medium. Däremot kunde en statistiskt signifikant effekt hittas i minskningen av variabiliteteten av xenografter med Gelatin som injicerings media. Minskning i felmarginalen orsakad av individuell variation, minskar mängden zebrafiskembryo som måste injiceras för att åstadkomma den nödvändiga mängden lyckade xenografter, vilket ur framför allt etisk synpunkt är en betydande fördel. Minskad variation inom screeningsgrupperna, och möjligheten att minska xenograft volymer ifall minde media läcker ut ur injiceringsstället, skulle också gagna möjligheterna för PDX-screening från små biopsier (begränsat antal cancerceller till förfogande) för att kunna kartlägga behandlingsalternativ innan mer invasiva operationer eller tunga behandlingar påbörjas.

I dagens läge anses synergistiskt verkande multidrog terapier som det mest lovande tillvägagångsättet för effektiv vård och eliminering av tumörer inom cancervård. Med tanke på det ökade intresset för transnationell biomedicin och etiska samt ekonomiska frågor, kunde zebrafiskcancermodellen väl utgöra ett potent hjälpmedel för allt snabbare vårdbeslut inom klinisk sjukvård, genom screenings på PDX biopsier i nära framtid.